Estimation of Big Thompson Flood Rainfall Using Infrared Satellite Imagery

By

Dennis E. Bielicki
and
Thomas H. Vonder Haar

Department of Atmospheric Science
Colorado State University
Fort Collins, Colorado

Colorado State University

Department of Atmospheric Science

Paper No. 300

ESTIMATION OF BIG THOMPSON FLOOD RAINFALL USING INFRARED SATELLITE IMAGERY

by

Dennis E. Bielicki and Thomas H. Vonder Haar

Department of Atmospheric Science

Colorado State University

Fort Collins, Colorado

December, 1978

Atmsopheric Science Paper No. 300

ABSTRACT

During the evening hours of 31 July 1976 heavy precipitation fell along the Colorado Front Range resulting in flash flooding in the Big Thompson Canyon causing the death of 139 people with 35.5 million dollar damage. This report utilizes GOES-1 infrared (IR) imagery to estimate the heavy convective precipitation during the Big Thompson Flood.

Analysis of the IR imagery prior to the Big Thompson storm showed that the thunderstorm complex formed at the intersection of frontal and orographic convective lines. A technique is developed to overlay the drainage basins onto the satellite imagery using the All Digital Video Imaging System for Atmospheric Research (ADVISAR) which included corrections due to the satellite sensing cloud tops.

The Scofield-Oliver satellite-derived precipitation estimation scheme was modified to reduce the precipitating portion of the cloud to 15 percent of the cloud defined by the 242^{o} K isotherm. IR imagery alone was used to identify overshooting domes which correlated well with areas of heavy precipitation. The computed area averaged precipitation for the Big Thompson Basin was 9.6 percent less than ground truth. Digital-video manipulation on the ADVISAR can indicate areas of heavy precipitation for IR satellite data on a real time basis.

TABLE OF CONTENTS

LIST OF TABLES

LIST OF FIGURES

Figure

1.0 INTRODUCTION

Beginning the evening of 31 July 1976 and continuing through 1 August 1976, heavy precipitation fell on the Big Thompson Drainage Basin along the Front Range in northern Colorado. The resulting flash flood through the narrow Big Thompson Canyon caused the death of 139 people with 35.5 million dollars damage. On 19-20 July 1977, heavy rainfall caused extensive flooding in the Johnstown, Pennsylvania area resulting in the death of 77 persons. In each case, the extensive flooding was caused by heavy rainfall from convective clouds. It is the intent of this report to develop a reliable method to estimate heavy precipitation to aid in the prediction of flash flooding.

Hughes and Longsdorf (1978) have published guidelines for flash flood predictions used by the National Weather Service Offices. With knowledge of soil conditions, basin configuration and river stage, the amount of three-hour area-averaged rainfall that will produce flash flooding is forecast. The key to this scheme is an accurate determination and three-hour forecast of area-averaged rainfall.

Radar itself is not a reliable indicator as radar derived precipitation figures underestimated rainfall during the Big Thompson flood by as much as 230 mm (9 in) as reported by Maddox, et al. (1977). Raingages also do not reflect true area precipitation mainly due to the randomness of convective activity. The same can be said for civilian "spotter" networks which don't present reliable information on average area precipitation. This study will examine the use of infrared (IR) satellite images to infer rainfall amounts.

Early attempts to estimate rainfall from geosynchronous or polar orbiting satellites were not very accurate as only visible data was available from the geosynchronous Applications Technology Satellites (ATS) and the polar orbiting satellites provided only two images per day. With the launch of the Synchronous Meteorological and Geostationary Operational Environmental Satellites (SMS/GOES) both higher resolution visual and infrared images were available at 30 minute intervals. However, precipitation estimation schemes were mainly confined to the tropics where cloud properties and environmental air are much different than those found in mid-latitudes.

The most promising satellite image inferred precipitation estimation scheme to date was developed by Scofield and Oliver (1977a). The technique uses both visual and IR data to determine half-hourly rainfall based on cloud growth and cloud top temperature.

This paper modifies the Scofield-Oliver technique and applies it to the infrared satellite images of the Big Thompson flood. The purpose of this study is to determine whether satellite rainfall estimates from IR data alone can be a reliable indicator of area precipitation and thus, be used in the prediction of flash floods.

The digitized satellite data was processed and analyzed on the All Digital Video Imagery System for Atmospheric Research (ADVISAR) developed by the engineers and atmospheric scientists at Colorado State University. The system allows for digital-video manipulation of the IR satellite data.

This report describes briefly the important synoptic conditions prior to the Big Thompson flash flood and summarizes the conditions indicative of heavy rainfall potential. Infrared satellite images leading up to the flood are examined and the location of the large thunderstorm

complex over the Big Thompson drainage is predicted through techniques developed by Purdom (1976).

The method used to navigate the satellite images is described along with the development and overlay of the drainage areas including the Big Thompson. Due to the earth's curvature and the satellite sensing cloud tops, clouds are apparently displaced from their actual position on earth. Calculations are developed to correct for this error to properly navigate the clouds within the drainage area overlay.

In the final section, the Scofield-Oliver rainfall estimation technique is modified and applied to the Big Thompson thunderstorm complex. The modifications include limiting the precipitating area to a smaller portion of the cloud and determining the location of overshooting tops by IR imagery alone. The hourly and cumulative area-averaged rainfall amounts computed in this study are compared to results by Woodley, et al. (1978) and ground truth as determined by gage-adjusted radar provided by Caracena, et al. (1978).

2.0 CASE STUDY 31 July - 1 August 1976

2.1 Synoptic Situation

Beginning the evening of 31 July 1976 and continuing into the early morning on 1 August 1976, extensive flash flooding occurred along the Rocky Mountain Front Range from the Big Thompson drainage in Colorado northward into Wyoming. Maddox, et al. (1977) and Simons, et al. (1977) extensively analyzed the meteorological aspects of the flash flooding. Figures 2-1 thru 2-4 are from Maddox's report.

Figure 2-1 is the surface analysis at 0000 GMT, 1 August 1976. Important features are a low pressure system over northwestern Colorado and a high pressure system on the Colorado-New Mexico border. A cold front moving from the northeast has overtaken a stationary front lying from Missouri through northeast Colorado and into Montana and gone stationary. A large high pressure system is centered in Canada with ridging behind the front into northeast Colorado. Immediately behind the front are high dewpoints $\geq 65^{o}F$ (shaded area) and strong southeast to northeast surface winds advecting the moisture into northeastern Colorado almost perpendicular to the Front Range. The old stationary frontal boundary across central Colorado is dissipating. Additionally, a squall line from Nevada to Utah is moving towards the northeast into southwest Wyoming.

The 500 millibar analysis at 0000 GMT 1 August 1976, Figure 2-2, shows high pressure centered over northern Texas with ridging extending across northeastern Colorado into Montana. A large band of moisture (shaded area) with dewpoint depression $\leq 6^{o}C$ lies from Nevada through Missouri and extends down into New Mexico. A short wave trough lies in southwestern United States moving towards the northeast. Maddox, et al.

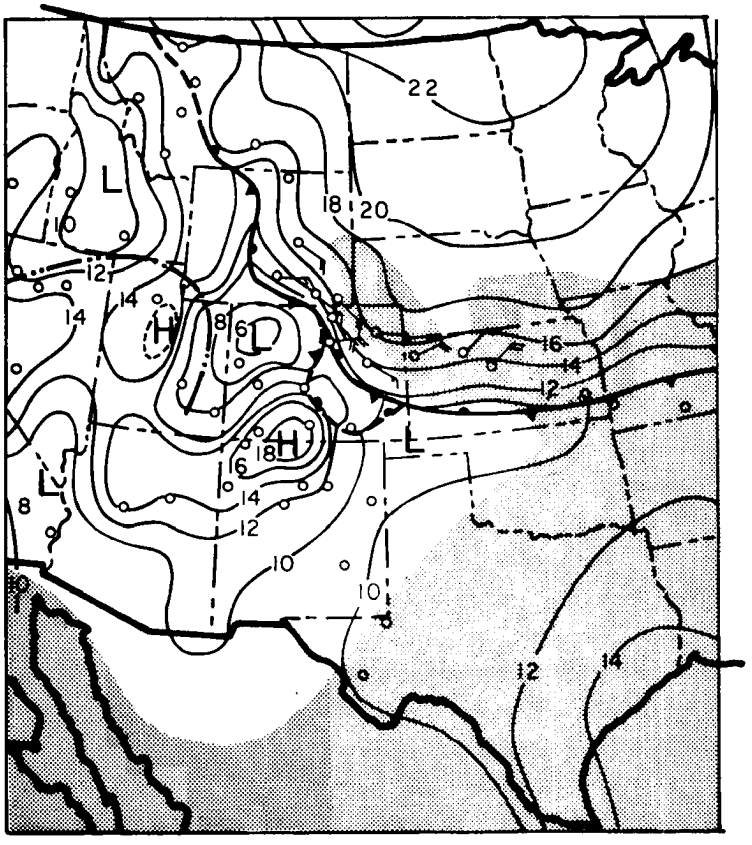

Figure 2-1 Surface analysis 1 August 1976 0000 GMT (from Maddox, et al., 1977). Dewpoint temperatures $\geq 65^{o}F$ are shaded.

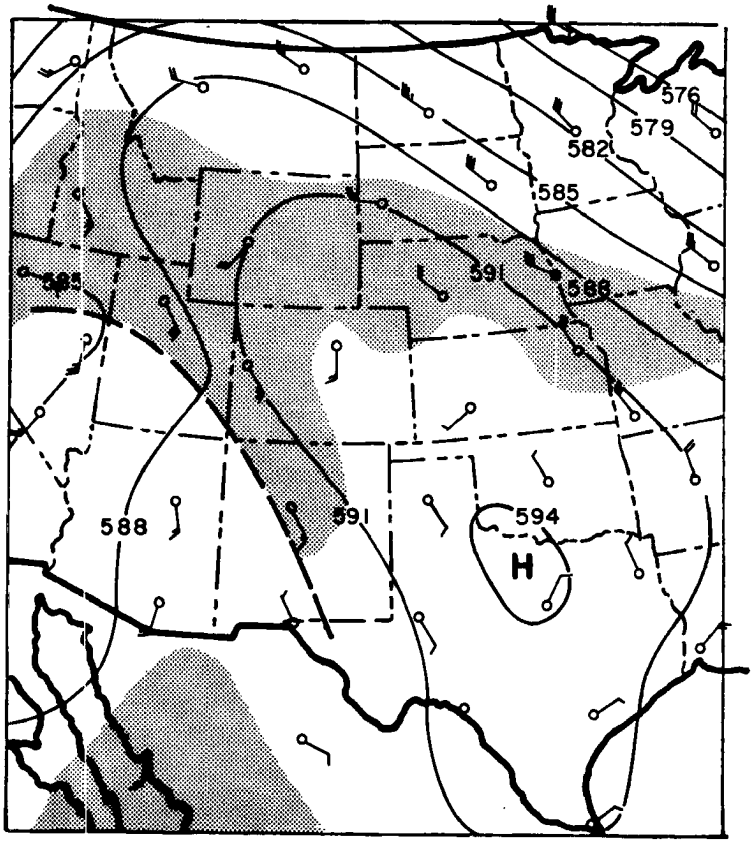

Figure 2-2 500 millibar analysis 1 August 1976 0000 GMT (from Maddox, et al., 1977). Dewpoint depression $\leq 6^{o}C$ is shaded.

point out that strong southerly winds are advecting moisture from the Gulf of California to Utah. Northeastern Colorado is under the ridge with light southerly winds and abundant moisture through 500 millibars.

Figure 2-3 is the 300 millibar analysis at 0000 GMT, 1 August 1976. Again, there is high pressure centered over the Kansas-Oklahoma border with ridging over northeastern Colorado. Strong southerly flow exists from the Gulf of California to Nevada leading into a moist area (shaded) of dewpoint depression $\leq 10^{o}C$.

Figure 2-4 is the Skew T/Log P plot of the upper air sounding over Sterling, Colorado at 1920 GMT, 31 July 1976. The Sterling soundings were taken in conjunction with operations of the National Hail Research Experiment (NHRE). Maddox, et al. feel that this sounding typifies the air mass behind the cold front associated with heavy precipitation along the Front Range. Their analysis indicates an unstable Lifted Index of -4 with a strong temperature inversion at 720 millibars. Precipitable water is 3.34 cm (1.31 in) from the surface to 500 millibars. Surface winds were moderate southeasterly with winds aloft generally light southeast-southwesterly.

Thus, the conditions were available for heavy precipitation as summarized by Maddox, et al.:

1. Strong easterly surface flow beneath a strong inversion behind a nearly stationary front carried moist conditionally unstable air into the Front Range.

2. Orographic lifting triggered the extensive thunderstorm complex.

3. Weak south-southeasterly winds aloft allowed the complex to remain nearly stationary.

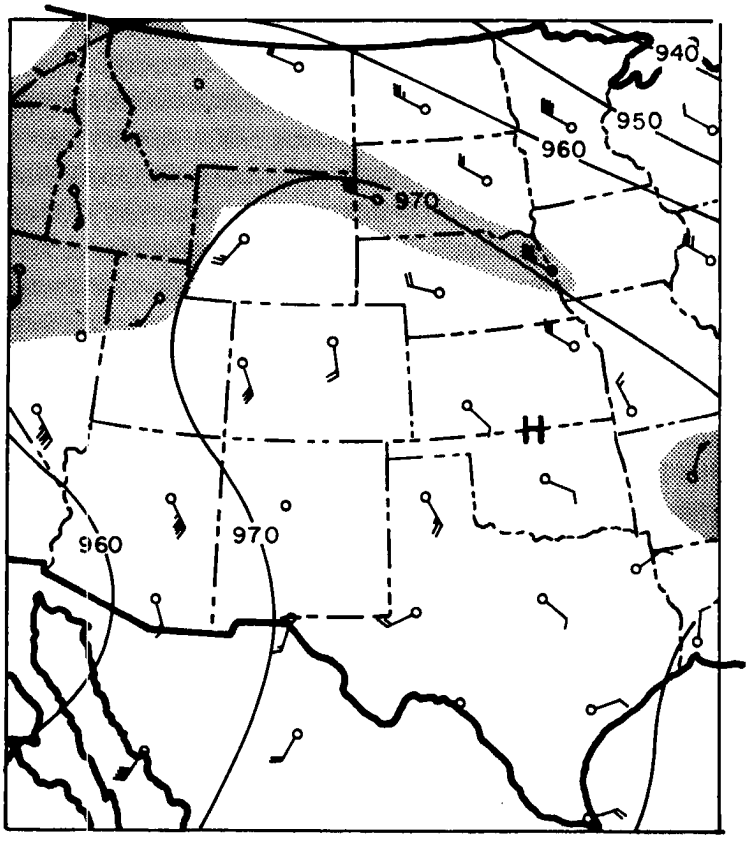

Figure 2-3 300 millibar analysis 1 August 1976 0000 GMT (from Maddox, et al., 1977). Dewpoint depression $\leq 10^{o}C$ is shaded.

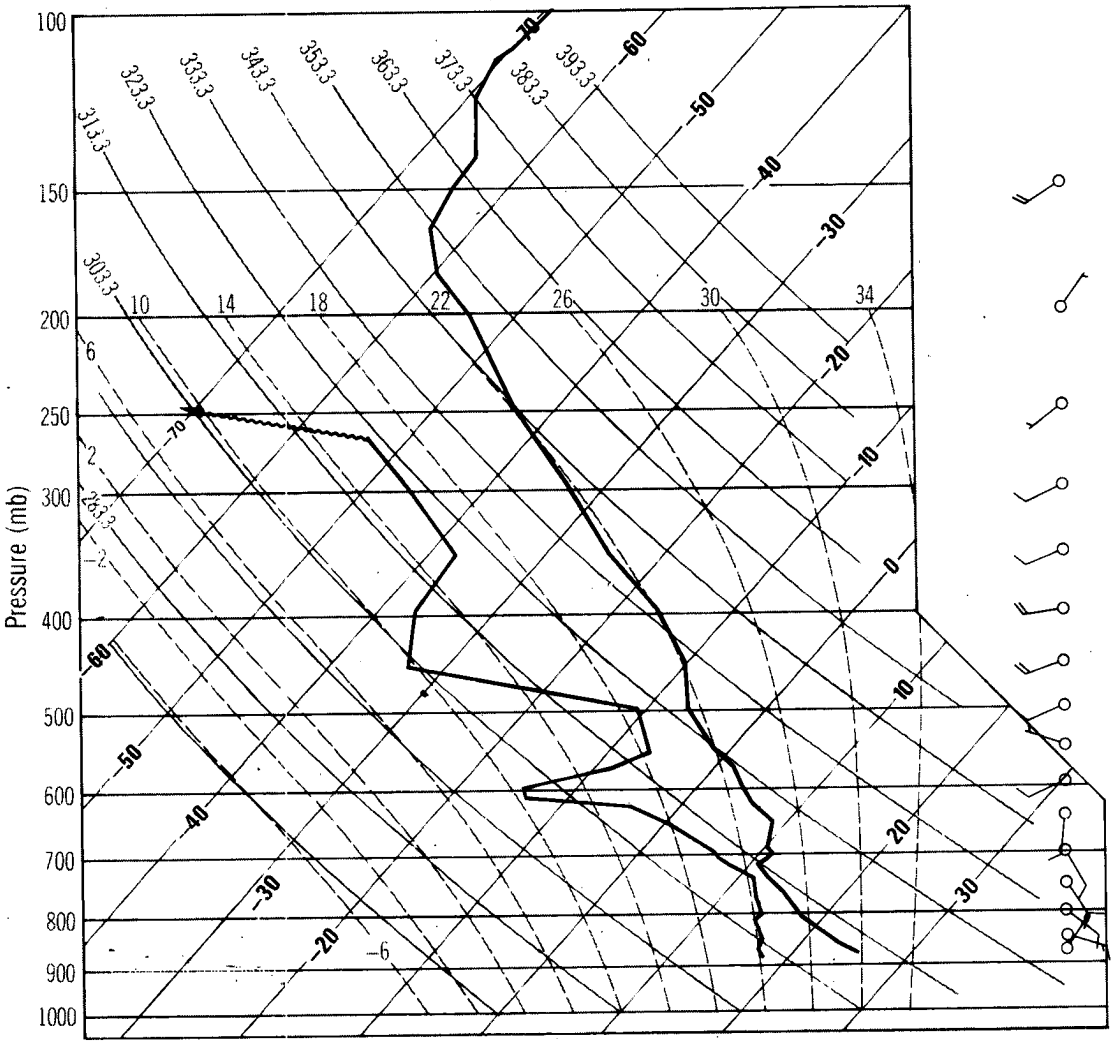

Figure 2-4 Skew T/Log P plot of Sterling, Colorado upper-air sounding taken at 31 July 1976 1920 GMT (from Maddox, et al., 1977).

2.2 Satellite Images

Digital satellite data for 31 July - 1 August 1976 used for this study was obtained from the National Space Science Data Center and the National Oceanic and Atmospheric Administration Environmental Research Laboratory. The data was recorded from the GOES-1 geostationary satellite located over the equator at 75^{o} W longitude. The satellite sensing instrument is the Visible Infrared Spin-Scan Radiometer (VISSR) which contains eight visible channels in the 0.55 to 0.70 μm band and one infrared (IR) channel operating in the 10.5 to 12.6 μm band. Further details of GOES satellite are given by McKowan (1975). Only the IR data was used for this study since the main period of interest occurred after dusk.

The data was processed on the All Digital Video Imaging System for Atmopsheric Research (ADVISAR) at Colorado State University (CSU). The ADVISAR is a combination of hardware and software components that allows for digital-video manipulation of satellite imagery. A detailed description of the ADVISAR is given by Brown (1978).

Infrared satellite images prior to the Big Thompson storm are shown in Figures 2-5 thru 2-8. The whitest gray shades indicate the coldest temperatures and consequently, the highest cloud tops. The resolution of the IR image from the geosynchronous satellite is 8 km (4.3 nm) over the subpoint.

Figure 2-5 is the IR image at 2100 GMT, 31 July 1976. A sparse amount of convective activity has formed along the east-west front in eastern Colorado and western Kansas. Orograhically produced convective clouds are oriented north-south along the Front Range. The clouds in this region are circular indicative of low shear environment and are moving north at 10 knots or less.

Figure 2-5 GOES-1 infrared image 31 July 1976, 2100 GMT.

Figure 2-6 GOES-1 infrared image 31 July, 1976, 2200 GMT.

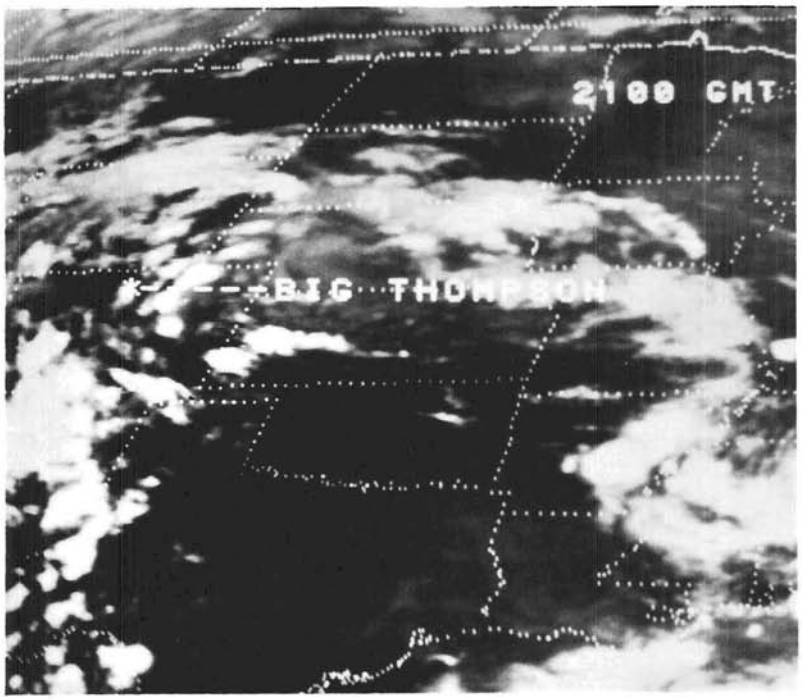
2100 GMT
BIG THOMPSON

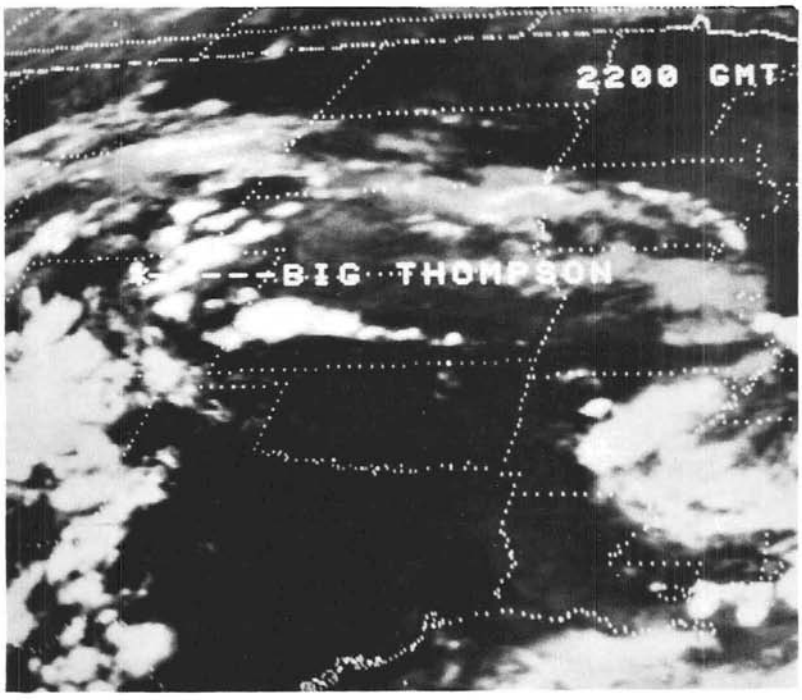
2200 GMT
BIG THOMPSON

By 2200 GMT, Figure 2-6, the east-west line is rapidly intensifying and expanding into eastern Kansas. Radar indicates a top of 17 km (56,000 ft) MSL along the Kansas-Colorado border.

Figures 2-7 and 2-8 are the 2300 and 2330 GMT images. The east-west line associated with the cold front has further intensified with numerous cells in Colorado and Kansas reaching to 13.4-16.2 km (44,000-53,000 ft) MSL. Additionally, the line has extended into Missouri. The north-south line also has enhanced convective activity. Purdom (1976), using high resolution visible imagery, found that intense convective activity will occur at the intersection of convective lines. If the convective clouds are large enough to be detected by the IR sensor, the lower resolution IR image could also be used to detect the merger.

Examining the 2330 GMT image, Figure 2-8, one would expect intense convective activity at the intersection of the orographically produced north-south line and the frontal east-west line. This is the point where the Big Thompson thunderstorm complex formed approximately one hour later. With weak vertical shear, weak steering current, and abundant moisture supply; a vertical precipitation efficient thunderstorm complex remained stationary over the Big Thompson Basin until 0400 GMT.

2.3 Severe Weather

Maddox, et al. reported that precipitation amounts exceeded 305 mm (12 in) with most falling between 0030 and 0430 GMT on 1 August 1976. Significant flooding occurred along the Big Thompson River and also along the North and South Forks of the Cache La Poudre River.

Figure 2-7 GOES-1 infrared image 31 July 1976 2300 GMT.

Figure 2-8 GOES-1 infrared image 31 July 1976 2330 GMT.

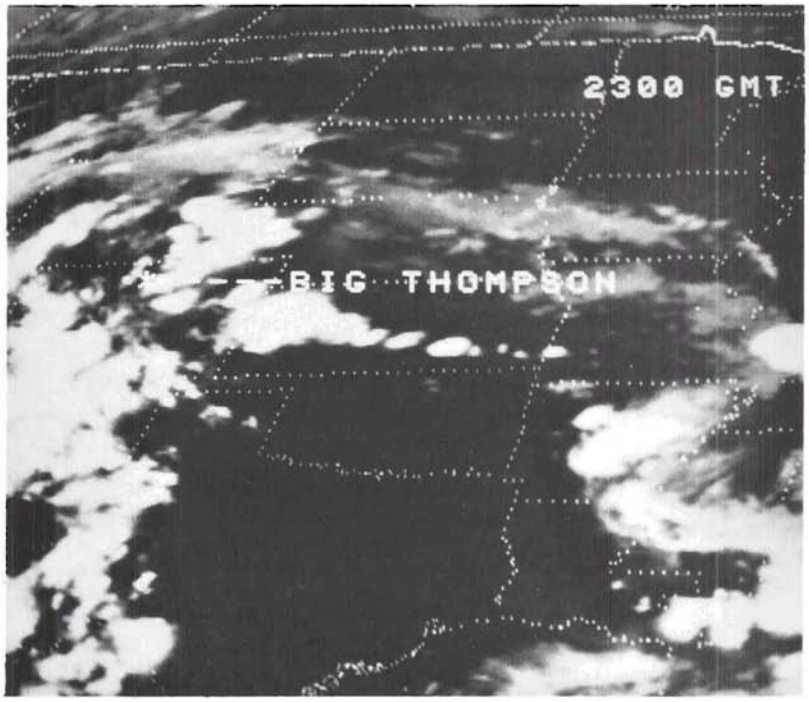
2300 GMT
BIG THOMPSON

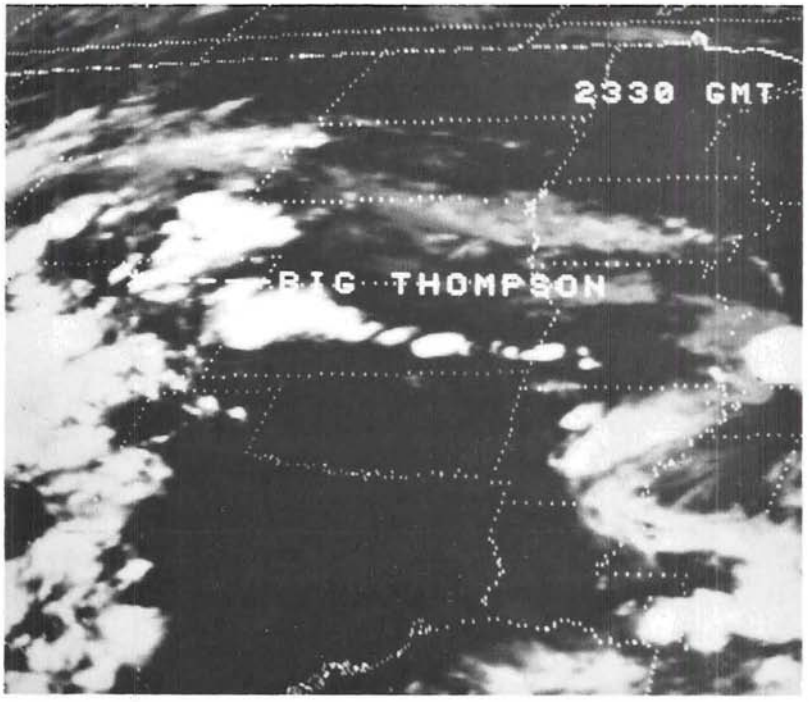
2330 GMT
BIG THOMPSON

3.0 NAVIGATION

Proper navigation of satellite images has varying degrees of importance. In studies of individual cloud growth and movement, absolute navigation of satellite images to the earth may be of little importance. However, when satellite image derived precipitation estimates are to be compared to ground truth, absolute navigation is extremely important.

The area of the Big Thompson Drainage Basin to the mouth of the canyon is 790 km^2 (305 mi^2) but the heaviest precipitation that produced the flash flooding fell in an effective drainage area of approximately 155 km^2 (60 mi^2) as reported by Grozier, et al. (1976). The area of the geostationary satellite IR pixel over this region is approximately 48 km^2 (18.5 mi^2), thus, small errors in navigation could easily mislocate the area of heaviest precipitation determined from satellite images.

3.1 Satellite Images

3.1.1 Image registration

The first step in the image navigation process involves relative navigation from one satellite image to another. The 1 August 1976 0130 GMT image was used as the basis for the image registration as it represented conditions during the period of heaviest precipitation.

The 0130 GMT satellite image was recorded on one of the ADVISAR's eight memory planes and displayed on the video monitors in order to select a landmark for the navigation process. If high resolution visual data is used, rivers or small reservoirs near the area of study are commonly used for landmarks. However, when only IR data is available, the landmark will normally be a larger body of water that exhibits a marked temperature contrast with the surrounding land. The best landmark on the 0130 GMT image was the center of Lake Winnebago, Wisconsin. In

the event that Lake Winnebago was obscured by clouds, the southern tip of Lake Michigan was selected as a secondary landmark. An electronic cursor was positioned over the landmark and the line-element coordinates recorded.

This procedure was performed on all of the satellite images available for this study. Appendix A lists the difference in landmark position between the 0130 GMT image and the other images in lines (vertical) and element (horizontal).

As a check on the relative navigation, the images were shifted the appropriate number of lines and elements on the memory planes in order to collocate the landmark. Again, the cursor was placed over the landmark on the video monitor and the images of the eight memory planes looped. The relative navigation was proved as the landmark held stationary during the image looping.

3.1.2 Image navigation

In order to accurately determine area rainfall rates from the IR satellite images, it is necessary to precisely locate the drainage areas on the satellite images. A navigation program as described by Smith and Phillips (1972) was used for this purpose. The program converts earth latitude-longitude coordinates to satellite image line-element coordinates or vice versa. Only the former program was used on this study. The navigation program first establishes the satellite's position in space using the orbital parameters listed in Table 3-1. Then after entering both the latitude-longitude and line-element position of a landmark, the program determines the line-element location of any other landmark from its latitude-longitude.

Table 3-1

Orbital Parameters

Epoch Time	7607240000
Semi-Major Axis	42167.753 km
Eccentricity	0.000833
Inclination	0.376
Mean Anomaly	303.868^{o}
Argument of Perifocus	032.642^{o}
Right Ascension of Ascending Node	250.384^{o}
Right Ascension	33.429^{o}
Declination	-89.664^{o}

Using the 0130 GMT, 1 August 1976 image, the line-element position of Lake Winnebago centered at 44° 01' N, 88° 25' W was entered into the program. The drainage areas studied are located in a box between 40° 00' and 41° 51' N, 105° 00' and 106° 00' W. The latitude-longitude coordinates of the four corners of the box were entered into the program which predicted the line-element locations shown in Table 3-2.

Mille Lacs Lake, Minnesota centered at 46° 15' N, 93° 39' W and the southwest edge of Lake Winnipeg, Manitoba, Canada at 50° 26' N, 96° 57' W were used for verification. Navigation program predicted line-element locations were in agreement with measured line-element locations on the 0130 GMT image within one pixel.

3.2 Drainage Area Overlay

The drainage areas selected lie along the Colorado Front Range from the North Poudre Basin south to the St. Vrain River drainage. The drainage areas were defined by analysis of the ridge lines on the United States Geological Survey (USGS) maps by Woodley, et al. (1978) and are shown in Figure 3-1. The grid was photographed and then digitized using the ADVISAR and stored in one of the memory planes.

The stored grid is in the earth latitude-longitude coordinate system and must be transposed into the satellite coordinate system before overlaying onto the satellite images. The method used for this conversion was explained in Section 3.1.2 and the results listed in Table 3-2. These are the satellite image line-element locations for the latitude-longitude points of the four corners of the box enclosing the drainage area.

The electronic cursor in the ADVISAR was positioned over one of the four corners of the box stored in the memory plane and displayed on the

Table 3-2

Drainage Area Location

Latitude	Longitude	Line	Element
40° 00' N	105° 00' W	261	510
40° 00' N	106° 00' W	262	488
41° 15' N	105° 00' W	248	526
41° 15' N	106° 00' W	248	504

Figure 3-1 Drainage areas along Colorado Front Range (from Woodley, et al., 1978)

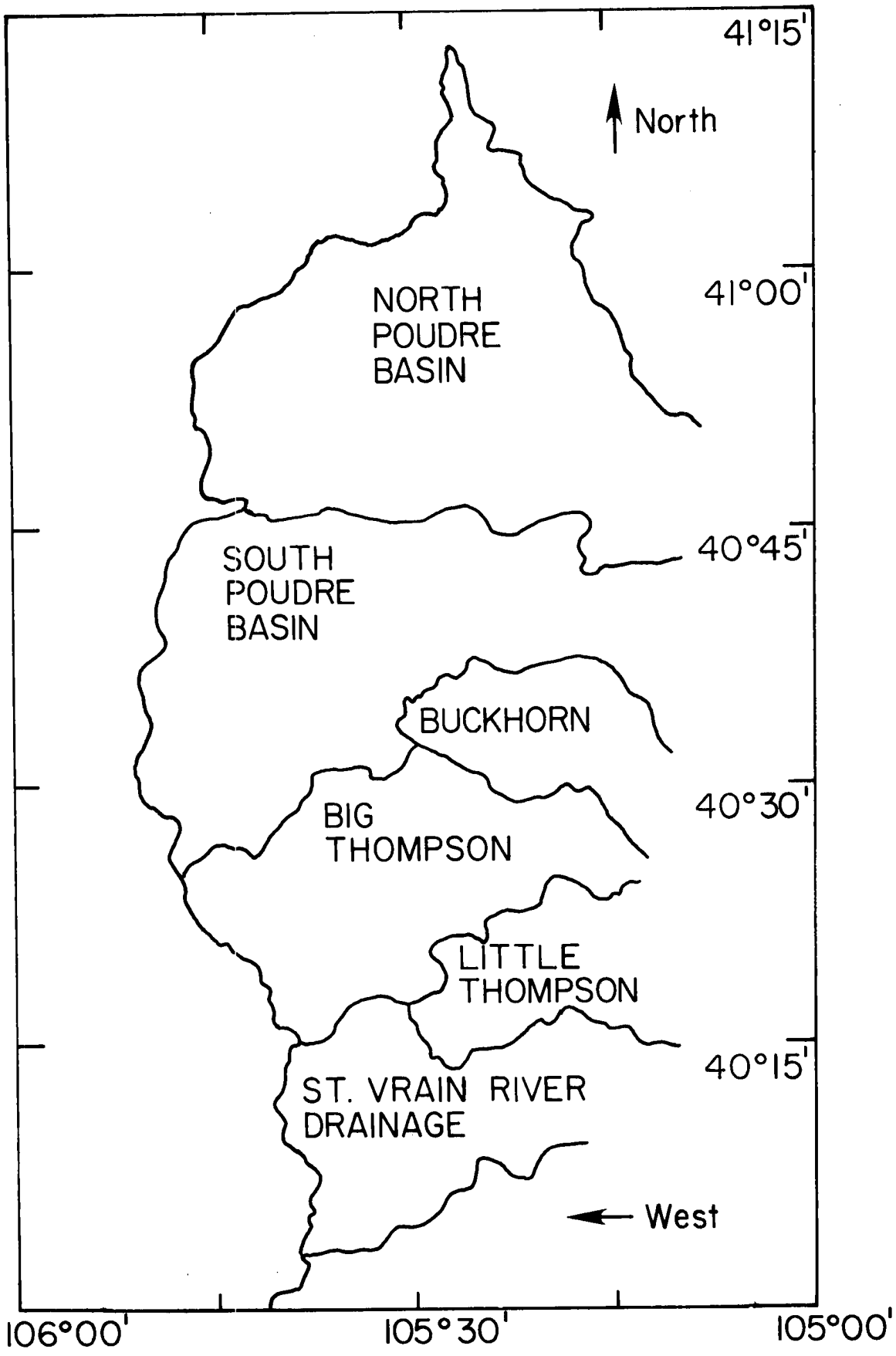
41°15'
North
41°00'
NORTH
POUDRE
BASIN
40°45'
SOUTH
POUDRE
BASIN
BUCKHORN
40°30'
BIG
THOMPSON
LITTLE
THOMPSON
40°15'
ST. VRAIN RIVER
DRAINAGE
West
106°00'
105°30'
105°00'

video monitor. The satellite line-element corresponding to the point was entered into the computer and the procedure repeated for the remaining three corners. A computer program then transposed the image within the box from the latitude-longitude coordinate system into the satellite line-element system and stored the grid on another memory plane. The transposed grid was transferred onto magnetic tape. Figure 3-2 shows the grid in the satellite coordinate system. The grid is now absolutely navigated and can be overlayed onto the satellite image for study.

3.3. Cloud-Height Correction

Before drainage area rainfall estimates are calculated from the satellite images, it is necessary to correct for cloud height. The geostationary satellite located over the equator senses cloud tops. Due to the earth's curvature, the cloud appears to be displaced away from the satellite sub-point. Figure 3-3 displays this error.

3.3.1 Method

This problem was examined by Pryor (1978) who established the following relationship:

$$d_c = h \tan Z_s \qquad (3\text{-}1)$$

where: d_c is the distance correction towards satellite subpoint

h is the cloud height

Z_s is the satellite zenith angle

To determine the correction in latitude and longitude for d_c examine figure 3-4

where: O is the center of the earth

S is the satellite subpoint

D is the cloud position

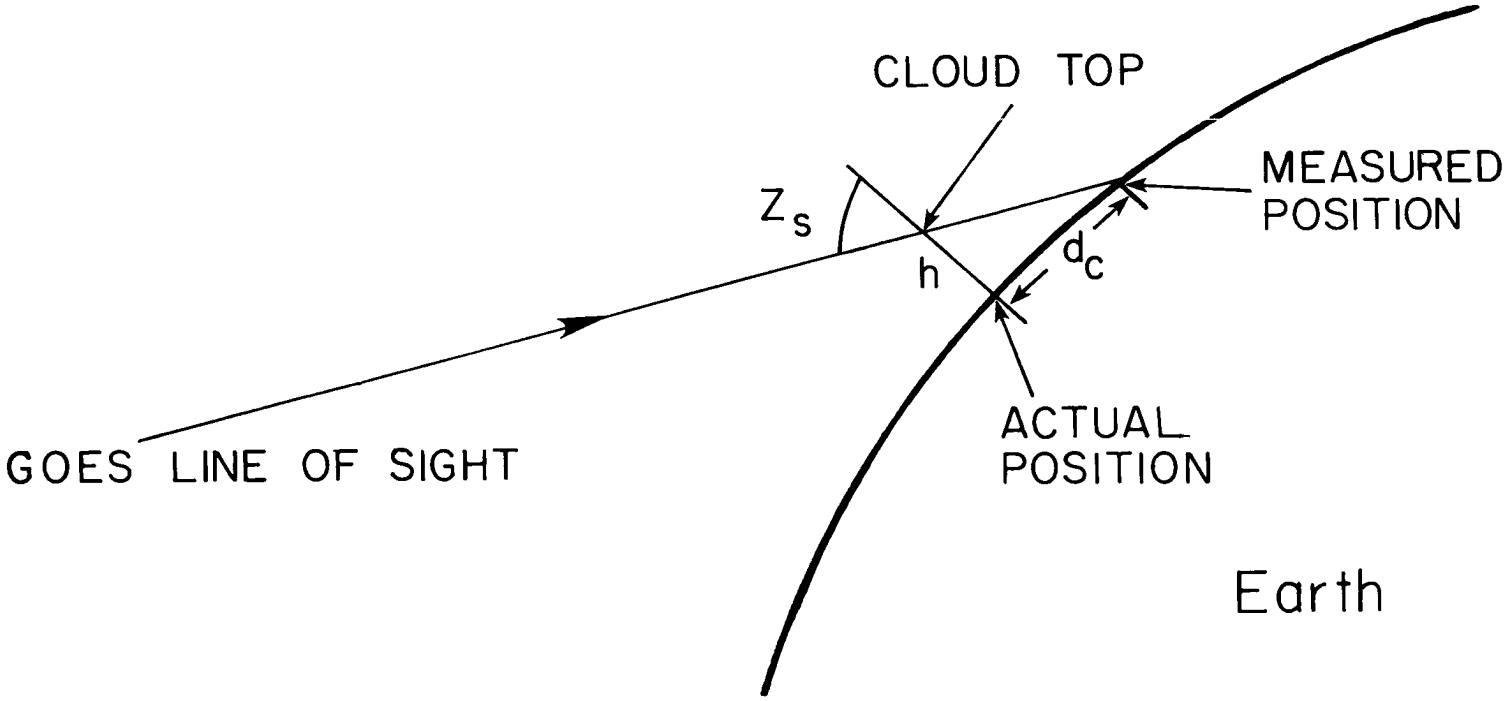

Figure 3-3 Depiction of error in location caused by satellite observation of cloud top (from Pryor, 1978).

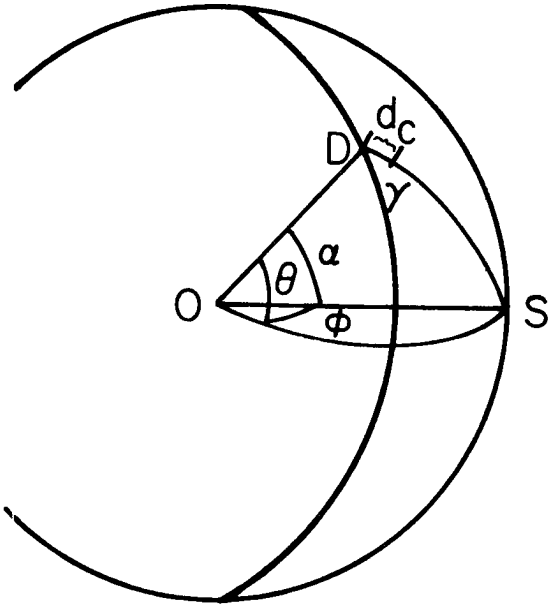

Figure 3-4 Satellite-Earth geometry

The distance correction (d_c) lies along lines DS. Using relationships for spherical right triangles :

$$\text{SIN } \gamma = \frac{\text{SIN } \phi}{\text{SIN } \alpha} \tag{3-2}$$

$$\text{SIN } (90 - \gamma) = \frac{\text{SIN } \theta}{\text{SIN } \alpha} \tag{3-3}$$

where: γ is the angle between the local longitude and line DS

ϕ is the local longitude

θ is the local latitude

Calculation of α is described by Pryor. The change in α ($\Delta\alpha$) due the distance correction is

$$\Delta\alpha = \frac{d_c}{OD} \tag{3-4}$$

where: OD is the earth radius.

The correction in latitude and longitude can be determined by again using the right spherical triangle rules:

$$\Delta\phi = \text{SIN}^{-1} [(\text{SIN } \gamma) \ (\text{SIN } \Delta\alpha)] \tag{3-5}$$

$$\Delta\theta = \text{SIN}^{-1} [\text{SIN } (90 - \gamma) \ \ \text{SIN } \Delta\alpha] \tag{3-6}$$

where: $\Delta\phi$ is longitude correction

$\Delta\theta$ is latitude correction

Finally,

$$\phi_c = \phi - \Delta\phi \tag{3-7}$$

$$\theta_c = \theta - \Delta\theta \tag{3-8}$$

with the subscript "c" indicating corrected values of latitude and longitude.

3.3.2 Results

Calculations were made to determine the correction for cloud height error at 40° 30' N, 105° 30' W which is located in the Big Thompson drainage. Using Pryor's equations, the satellite zenith angle (Z_s) for

this point is 56.17416°. Latitude-longitude correction calculations were made for cloud tops 14-20 km (46,000-65,000 ft) MSL and the results are listed in Table 3-3.

Maximum cloud tops determined by radar over the Big Thompson region were measured at 18.9 km (62,000 ft) MSL. Consequently, 11' 31" and 8' 48" corrections in latitude and longitude, respectively, were necessary to compensate for cloud height. The navigation program described in Section 3.1.2 was rerun for 40° 30' N, 105° 30' W and 40° 18' 29" N, 105° 21' 12" W. The difference between the two points was computed as two lines and one element. The satellite images should be shifted that amount towards the satellite subpoint for cloud height correction. Further calculations showed that the correction for cloud heights 16-20 km (52,500-65,500 ft) MSL is identical due to the coarseness of the IR pixel.

Table 3-3

Latitude-Longitude Corrections for Cloud Height

Cloud Height (h) (km)	(ft)	Distance Correction (d_c) (km)	Longitude Correction ($\Delta\phi$) (deg)	Latitude Correction ($\Delta\theta$) (deg)
14	46,000	20.8926	06' 51"	08' 57"
16	52,500	23.8772	07' 50"	10' 14"
18	59,000	26.8618	08' 48"	11' 31"
20	65,500	29.8465	09' 47"	12' 48"

4.0 RAINFALL ESTIMATES FROM SATELLITE IMAGES

Hughes and Longsdorf (1978) have established guidelines for flash flood predictions used by the National Weather Service offices. The guidelines combine information based on slope, soil moisture, permeability and basin size along with initial river stages to compute "Flash Flood Headwater Basin Crest Stage Guidances" (Basin Indexes) for numerous drainage basins. The "Basin Index" is a forecast of the basin area-averaged three-hour rainfall amount that will produce flooding. Using the "Flood Advisory Table" in conjunction with the "Basin Index", the amount and timing of the flood crest can be predicted. However, the key to this scheme is the accurate determination and prediction of three-hour area-averaged rainfall amounts.

Maddox, et al. (1977) showed that radar itself is not a reliable indicator of precipitation amounts as the Limon radar underestimated precipitation amounts during the Big Thompson Flood by as much as 230 mm (9 in). Raingages are not an accurate area precipitation indicator either due to the random distribution of convective cells. There definitely is a need for other methods to determine precipitation amounts. This study examines the possibility of using IR satellite images to accurately determine area-averaged rainfall amounts.

4.1 Previous Studies

Many studies have been accomplished to estimate rainfall from geosynchronous or polar orbiting satellites. Martin and Scherer (1973) summarize early attempts of indirect inference of convective clouds using either visible or infrared satellite imagery. Later studies have utilized geosynchronous satellite imagery due to its higher frequency

30 minute image intervals. Griffith and Woodley (1973) and Reynolds and Vonder Haar (1973) showed that bright clouds in the visible were thicker and thick clouds wetter. Martin and Sidkar (1973, 1974) and Griffith, et al.(1976) found that convective precipitation is more intense with growing clouds. Unfortunately, most of the above work was accomplished in tropical regions where cloud types are much different than those over the mid-latitudes. Microphysical properties, cloud bases, sub-cloud evaporation, environmental wind shear and moisture vary between the two regions.

Recently, two rainfall measuring techniques were applied over mid and western United States. Woodley, et al.(1978) applied their technique to the Big Thompson flash flood and their results are shown in Section 4.3.2. They developed an empirical, diagnostic technique relating time histories of convective clouds to rainfall using either visible or infrared satellite imagery. In the analysis of the Big Thompson, only infrared data was used with the 253^{o} K isotherm defined as the cloud threshold. Using the ratio of the cloud area to the maximum cloud area, the precipitation area for each cloud is calculated based on previous studies. An important consideration in this calculation is the growth trend as growing clouds precipitate more than dying clouds. Knowing the echo area and growth trend, rain volume is computed and allocated over the echo area according to coldest temperatures. A problem with the technique currently is that it requires complete history of cloud development. Consequently, the technique cannot be utilized on a real-time basis.

4.2 Scofield-Oliver Rainfall Estimation Technique

The most promising satellite rainfall estimation technique to date was developed by Scofield and Oliver (1977a) and utilizes both visual and infrared data from the geosynchronous satellites. Their technique predicts a real-time precipitation estimate from convective clouds over a point or station. Most of the data used to develop their precipitation estimation scheme came from central United States during the summer months. Their technique is divided into three parts:

1. Determining the active part of the convective system,
2. Making an initial estimate based on IR data alone,
3. Using both visual and IR data to determine areas of heavier rainfall.

Techniques used to determine the active portion of the convective cloud as put forth by Scofield and Oliver are shown in Table 4-1.

The second step makes an initial first guess of precipitation based on the half-hourly change in the coldest top temperature from digitally enhanced IR satellite images. The digitally enhanced curve (Mb) developed by the National Environmental Satellite Service (NESS) enhances the colder thunderstorm tops as explained by Scofield and Oliver (1977a). They concluded:

1. Cold tops in the IR which are expanding in areal coverage produce more rainfall than those not expanding.
2. Decaying clouds produce little or no rainfall.
3. Clouds with cold tops in the IR imagery produce more rainfall than those with warmer tops.

Table 4-1

Method to Determine Active Portion of Convective System
(from Scofield and Oliver, 1977a)

1. Tighest IR temperature gradient
2. Presence of overshooting top
3. Brighter and/or more textured anvil
4. Edge of anvil which moves least
5. 300 mb upwind end of anvil

4. Clouds with cold tops that are becoming warmer produce little or no rainfall.

Figure 4-1 quantifies the above guidelines. Two consecutive half-hour IR images are compared. If the coldest top temperature increases in size or decreases in temperature, significant precipitation is indicated by Figure 4-1. The amount is determined by the degree of expansion of the coldest top expressed in fractions of degrees of latitude. The scheme also allows for precipitation in clouds when the coldest tops show no change, decrease in area, or become warmer. However, precipitation amounts are significantly smaller. For example, if the coldest top was in the -62° C to -80° C range and increased in size by $\frac{1}{2}^{\circ}$ latitude during the half-hour, the half-hourly rainfall would be predicted as 19 mm (0.75 in) from figure 4-1. If the coldest cloud top temperature had decreased to -80° C over a length less than $1/3^{\circ}$ latitude, 12.7 mm (0.5 in) precipitation would be forecast.

The last step of the precipitation estimation scheme enhances the half-hourly precipitation by 12.7 mm (0.5 in) due to the presence of any of the following:

1. Overshooting tops
2. Merging cloud lines
3. Thunderstorm mergers.

Overshooting tops as shown by Fujita (1972) and Shenk (1974) are indicative of areas of strong vertical motion within a cloud causing the top to penetrate the cirrus anvil or tropopause. Severe weather, including heavy rainfall, has been associated with overshooting tops.

Merging cloud lines are indicative of areas of intense convection. This was shown by the work of Miller (1972) and later Purdom (1973, 1974, 1976). Merging cloud lines cause a convergence of low-level

CLOUD TEMPERATURE	COLDEST CLOUD INCREASED IN AREA OR BECAME COLDER			COLDEST CLOUD REMAINED THE SAME	COLDEST CLOUD DECREASED IN AREA OR BECAME WARMER
	>2/3° Lat	>1/3≤2/3	≤ 1/3		
Medium Gray (-32 to -41°C)	0.25	0.15	0.10	0.05	T
Light Gray (-42 to -52°C)	0.50	0.20	0.15	0.10	0.01
Dark Gray (-53 to -58°C)	0.75	0.40	0.20	0.15	0.03
Black (-59 to -62°C)	1.00	0.60	0.30	0.20	0.05
Repeat Gray Levels (-63 to -80°C)	1.50	0.75	0.40	0.30	0.08
White (Below -80°C)	2.00	1.00	0.50	0.40	0.10

Figure 4-1. Initial half-hourly rainfall estimate (from Scofield and Oliver, 1977a).

moisture enhancing convective development. Purdom showed that enhanced thunderstorm activity can result from merger of two convective lines or a convective line interacting with an "arc" cloud created from an existing thunderstorm. Simpson and Woodley (1971) and Woodley and Sax (1976) showed that increased rainfall resulted from thunderstorm mergers.

When the enhanced precipitation is added to the "first guess" obtained from Figure 4-1, rainfall over a certain point or station is determined. This scheme was then modified by Scofield and Oliver (1977b) and Scofield (1978) to determine area rainfall. Assuming that the coldest IR imagery contours are associated with the most active portion of the convective cloud and thus the heaviest rainfall, precipitation isohyets are drawn parallel to the IR temperature contours. Scofield (1978) found that isohyets representing $\geq$ 6.35 mm (0.25 in) should be drawn in a width of 16 km (10 mi) or less. Additionally, enhanced precipitation due to overshooting tops is concentrated in 8 km (5 mi) width.

4.3 Application of the Scofield-Oliver Precipitation Estimation Scheme

4.3.1 Method

The Scofield-Oliver precipitation scheme was applied to the Big Thompson flash flood utilizing IR satellite imagery displayed on the ADVISAR. Use of the ADVISAR provides for a more accurate determination of precipitation as $1^{o}K$ temperature differences can be resolved and the area of study enlarged for better resolution. In this study, the drainage area overlay and satellite images were enlarged four times with the IR temperatures color enhanced.

Initial application of the Scofield-Oliver scheme resulted in an unrealistically large area of precipitation when compared to the Limon

radar PPI display. Woodley, et al. (1978) established that only 10 percent of the cloud defined by the 253°K temperature contour was precipitating. In this case study, it was assumed that the precipitating portion of a cloud as defined by the 242°K contour occurred in the coldest 15 percent of the cloud area. This assumption produced a precipitation area that correlated well with the Limon radar PPI representations.

The second modification concerned the identification of overshooting tops by IR imagery only. Fujita (1974) differentiates between overshooting turrets and overshooting domes. Overshooting turrets are less than 1.6 km (1 mi) in diameter with an overshooting period of about four minutes. Since the size of an IR pixel in the area of study is 48 km^2 (18.5 mi^2), overshooting turrets would not be discerned by the sensor. Fujita defines overshooting domes as a conglomerate of turrets varying in diameter between 1.6 and 16 km (1 and 10 mi). Consequently, the larger domes would be sensed by the satellite. Shenk (1974) determined that the overshooting domes have a cycle of about 20 minutes. He noted that higher level cirrostratus associated with the overshooting domes persisted for approximately one hour in one case. The persistence suggested that there were surges of convective growth and decay within the area indicating intense updrafts within the convective cell. Identification of the domes or higher cirrostratus by the IR sensor allowed a precipitation amplification of 12.7 mm (0.5 in) over an area 5 km (8 mi) wide.

4.3.2 Results

The digitized satellite IR data used to determine the precipitation estimates was available only for 0000, 0100, 0130, 0200, 0330, 0500 and 0630 GMT on 1 August 1976. Additionally, the 0000 GMT image was

improperly calibrated and could only be used to determine cloud position. The Scofield-Oliver precipitation estimation scheme determines half-hourly rainfall amounts based on two consecutive half-hourly IR images. Consequently, the satellite images and rainfall estimates were interpolated in the Scofield-Oliver scheme.

Radar echoes from the Limon radar are shown in Figures 4-2 through 4-9. The figures display the location of the radar echoes transformed into the satellite coordinate system with the grid of the drainage basins superimposed. The solid line encloses the area of Video Integrator Processor (VIP) levels 1 and 2 with the shaded area indicating VIP level 3. The radar echo locations are from Maddox, et al. (1977) who calculated the gage-adjusted rainfall rate for VIP level 3 to be 150 mmh^{-1} (5.91 inh^{-1}). Notice that from 0132 to 0400 GMT, Figures 4-4 to 4-9, areas of VIP level 3 are centered over the Big Thompson Drainage Basin indicating the heavy precipitation over that region throughout the time period. The precipitation area shown in Figures 4-2 through 4-9 is located at the 200 km (125 nm) maximum range of the Limon radar, and the areas are cutoff abruptly when the range is exceeded. Since the echo area was located near the maximum radar range of a poorly calibrated radar, the radar underestimated precipitation by almost 230 mm (9 in) at Glen Comfort.

Figures 4-10, 4-12, 4-14, 4-16 and 4-18 are photographs of the color enhanced ADVISAR image of IR data with the drainage area overlay from 0100 to 0500 GMT, 1 August 1976. The black-body temperatures represented by the various colors are listed in Table 4-2. Note that the coldest temperatures represented by black and red are centered over the Big Thompson drainage from 0100 to 0330 GMT correlating well with

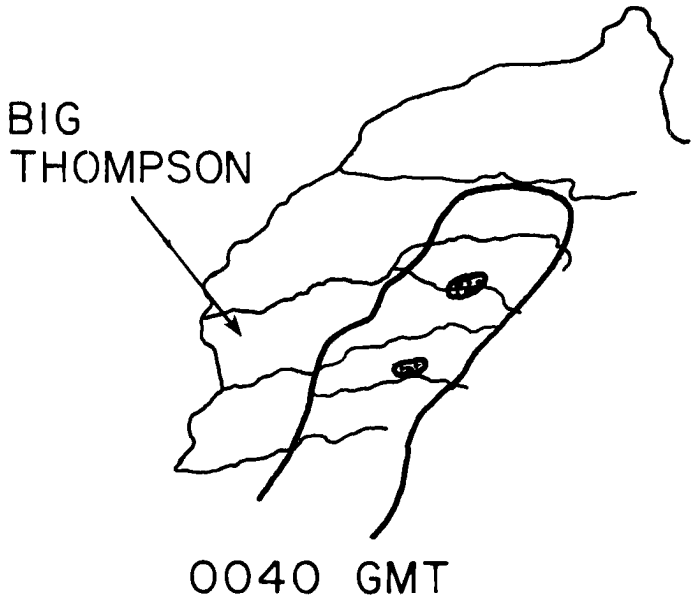

Figure 4-2 Limon radar echoes with drainage basins superimposed 1 August 1976 0040 GMT. Solid line enclosed VIP levels 1 and 2. VIP level 3 is shaded.

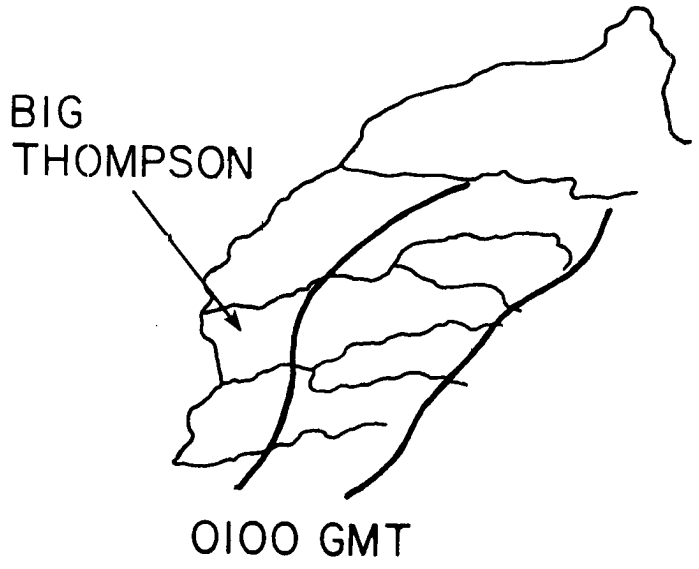

Figure 4-3 Limon radar echoes with drainage basins superimposed 1 August 1976 0100 GMT. Solid line encloses VIP levels 1 and 2.

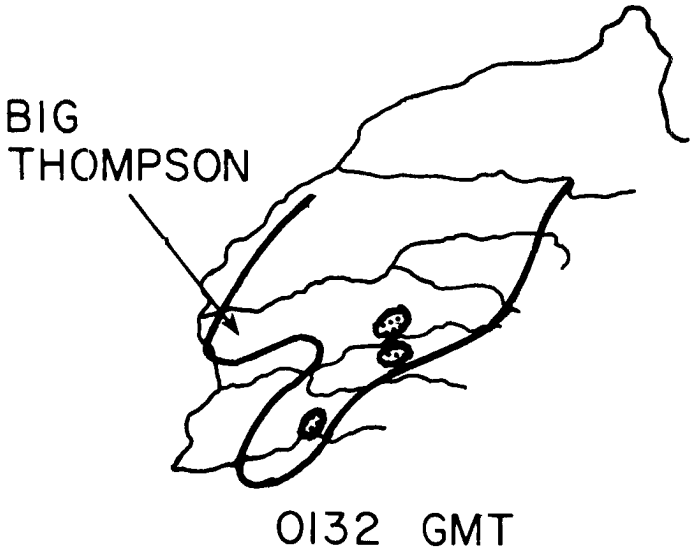

Figure 4-4 Limon radar echoes with drainage basins superimposed 1 August 1976 0132 GMT. Solid line encloses VIP levels 1 and 2. VIP level 3 is shaded.

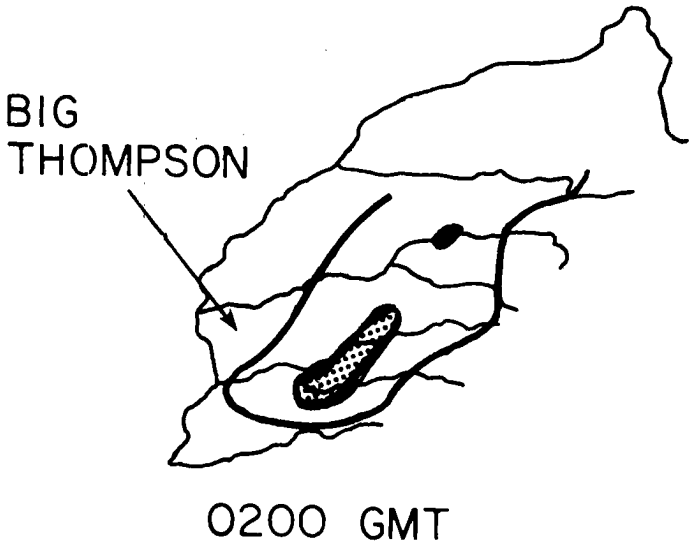

Figure 4-5 Limon radar echoes with drainage basins superimposed 1 August 1976 0200 GMT. Solid line encloses VIP levels 1 and 2. VIP level 3 is shaded.

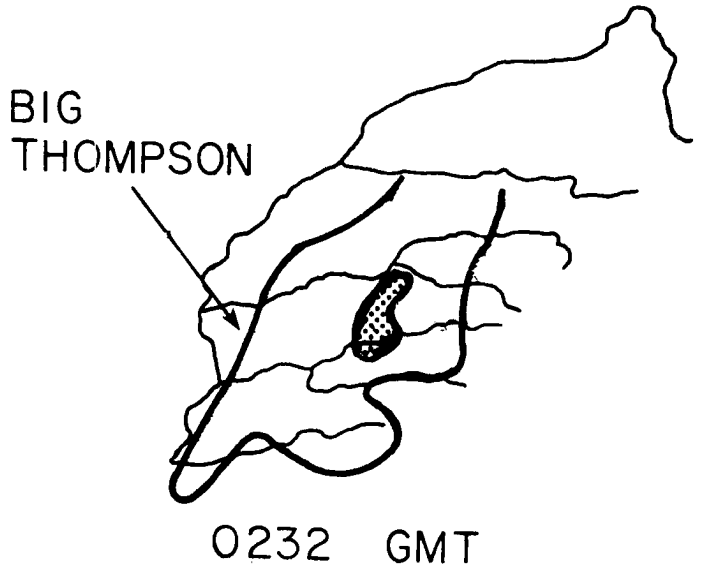

Figure 4-6 Limon radar echoes with drainage areas superimposed 1 August 1976 0232 GMT. Solid line encloses VIP levels 1 and 2. VIP level 3 is shaded.

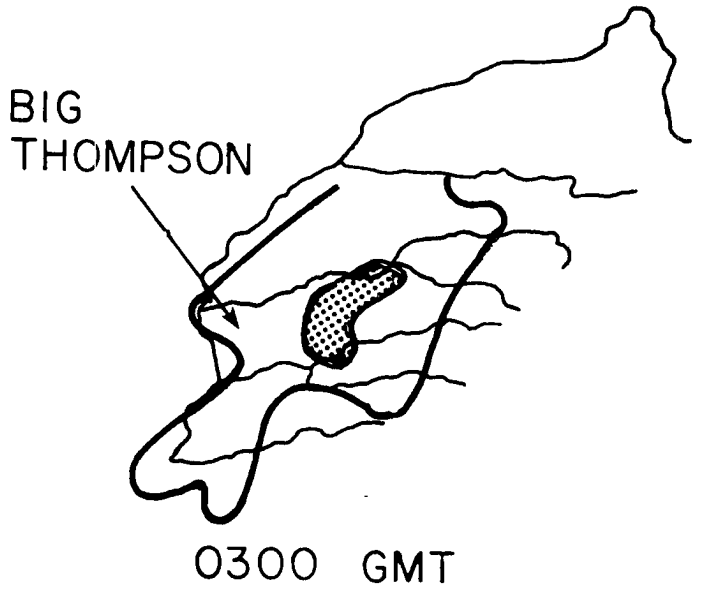

Figure 4-7 Limon radar echoes with drainage areas superimposed 1 August 1976 0300 GMT. Solid line encloses VIP levels 1 and 2. VIP level 3 is shaded.

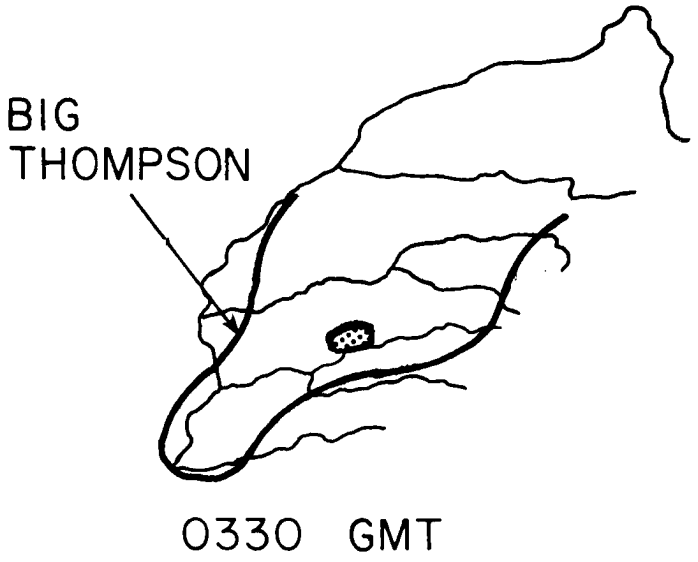

Figure 4-8 Limon radar echoes with drainage areas superimposed 1 August 1976 0330 GMT. Solid line encloses VIP levels 1 and 2. VIP level 3 is shaded.

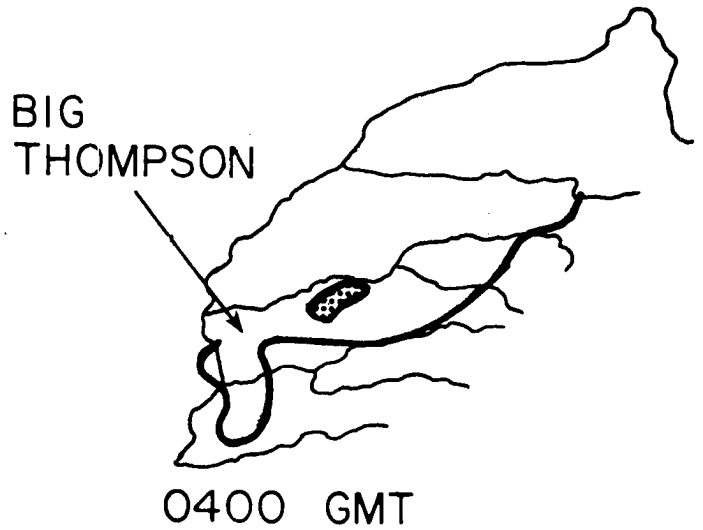

Figure 4-9 Limon radar echoes with drainage areas superimposed 1 August 1976 0400 GMT. Solid line encloses VIP levels 1 and 2. VIP level 3 is shaded.

Table 4-2

Legend of ADVISAR Enhancement Colors

Color	Black-Body Temperature (^{o}K)
Black	198
Red	199-200
Green	201-202
Blue	203-206
Yellow	207-210
Gray Shades	>210

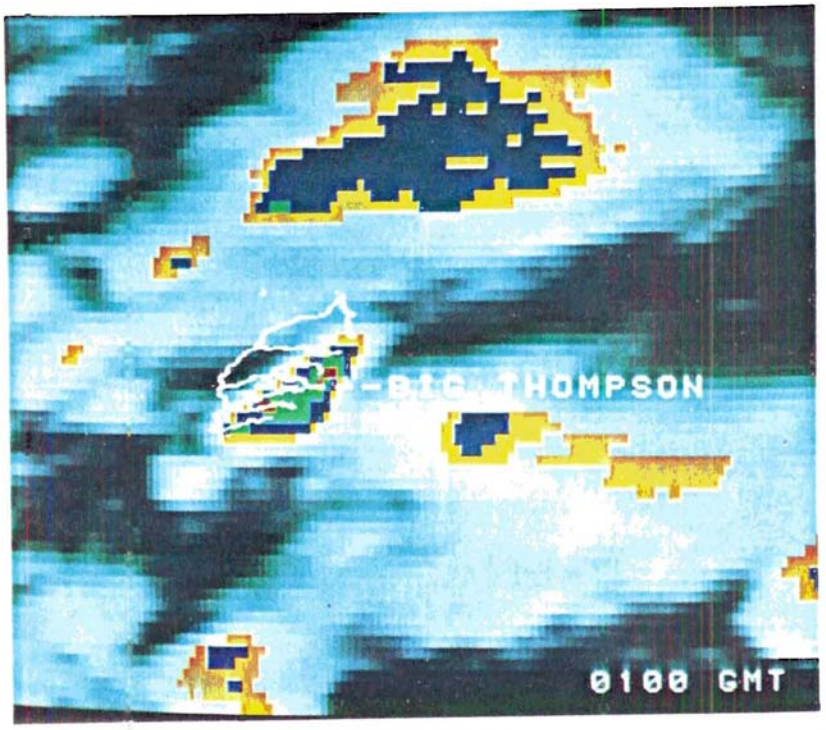

Figure 4-10 Infrared image 1 August 1976 0100 GMT with drainage area overlay.

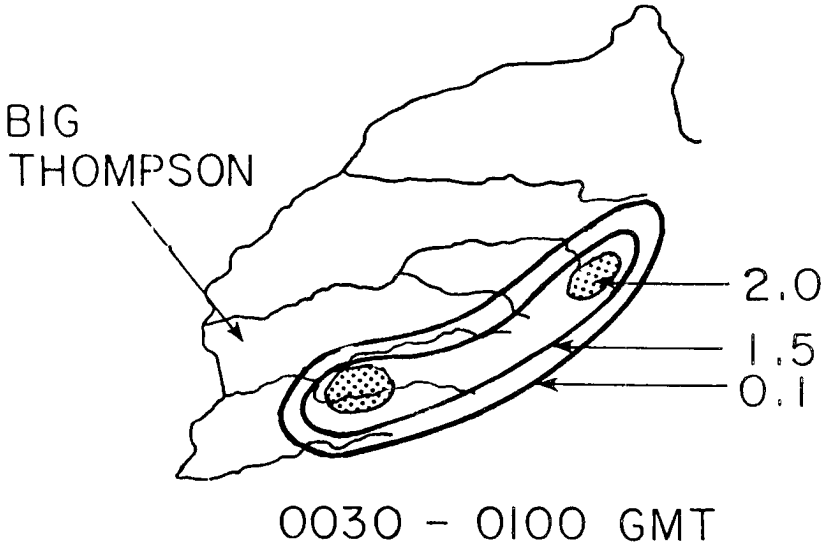

Figure 4-11 Satellite-derived half-hourly isohyet analysis (in), 0030-0100, 1 August 1976.

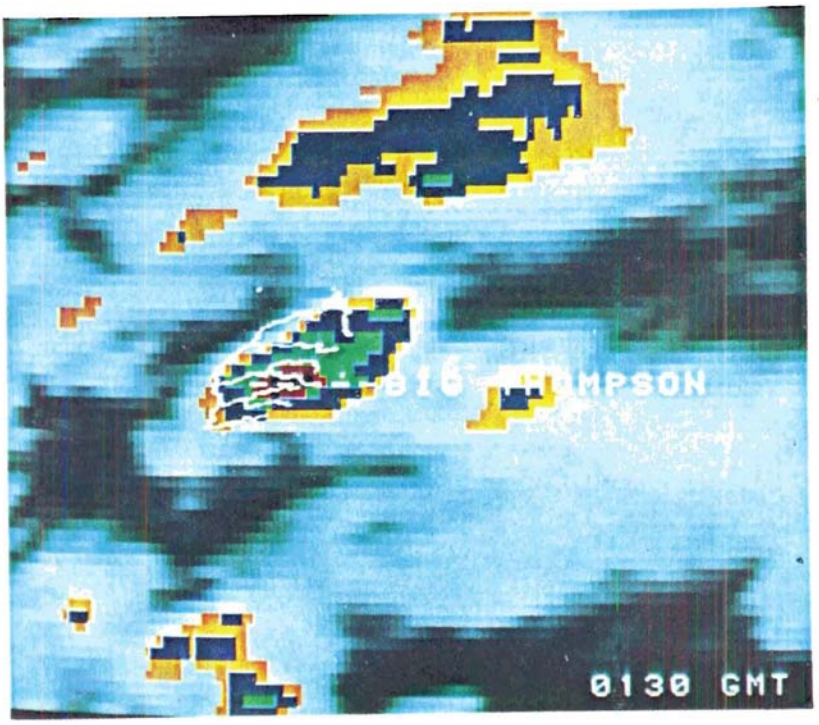

Figure 4-12 Infrared image 1 August 1976 0130 GMT with drainage area overlay.

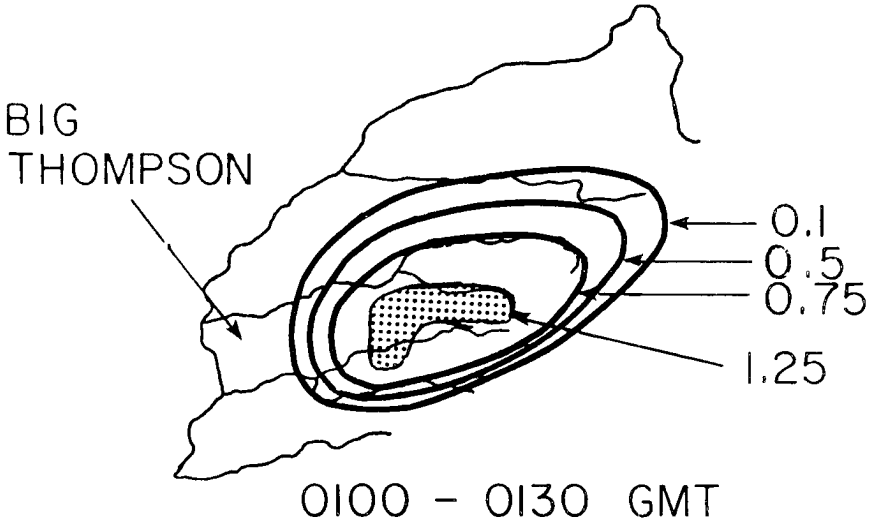

Figure 4-13 Satellite-derived half-hourly isohyet analysis (in), 0100-0130 GMT, 1 August 1976.

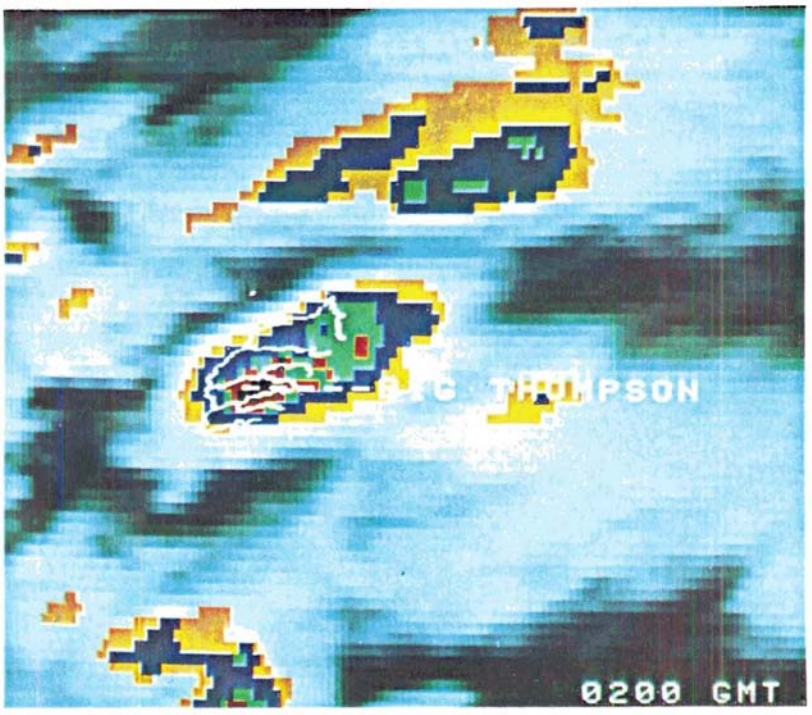

Figure 4-14 Infrared image 1 August 1976 0200 GMT with drainage area overlay.

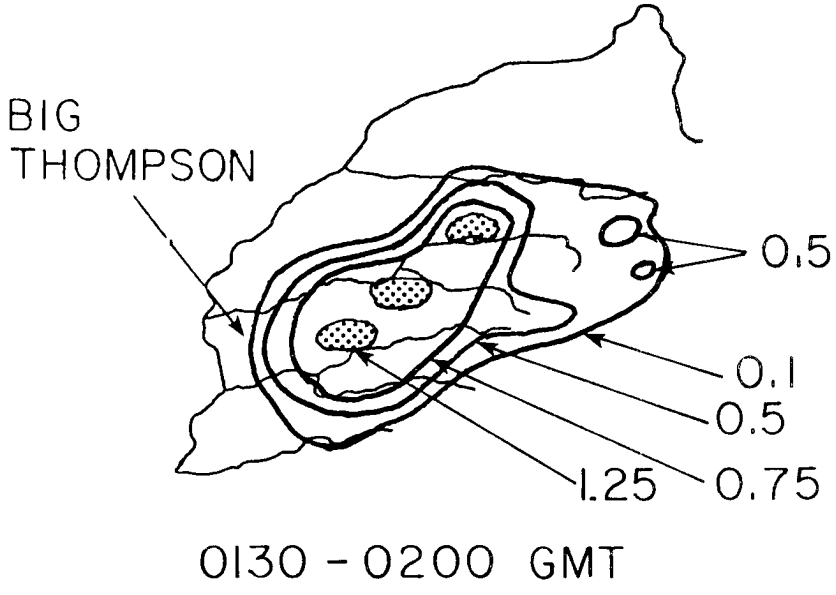

Figure 4-15 Satellite-derived half-hourly isohyet analysis (in), 0130-0200 GMT, 1 August 1976.

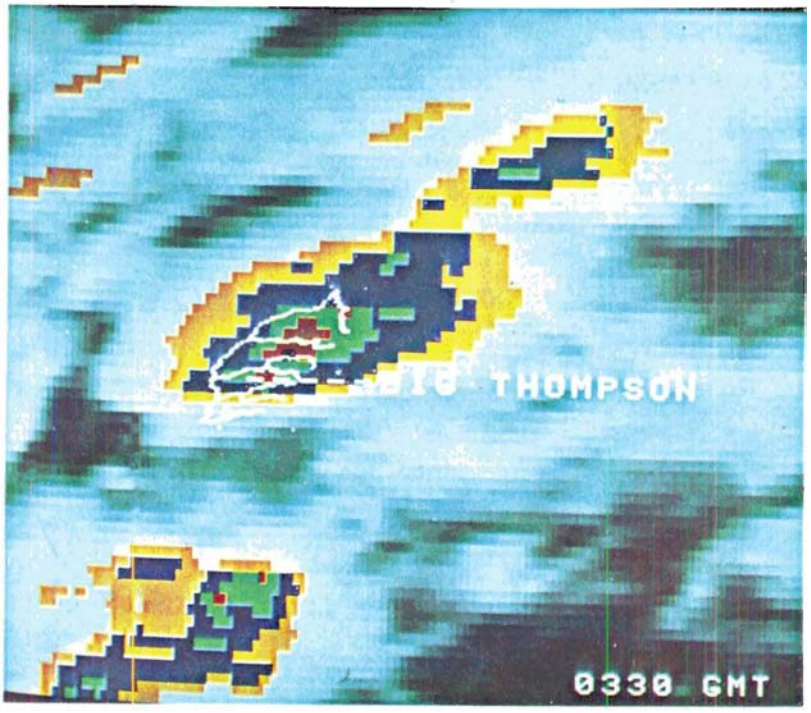

Figure 4-16 Infrared image 1 August 1976 0330 GMT with drainage area overlay.

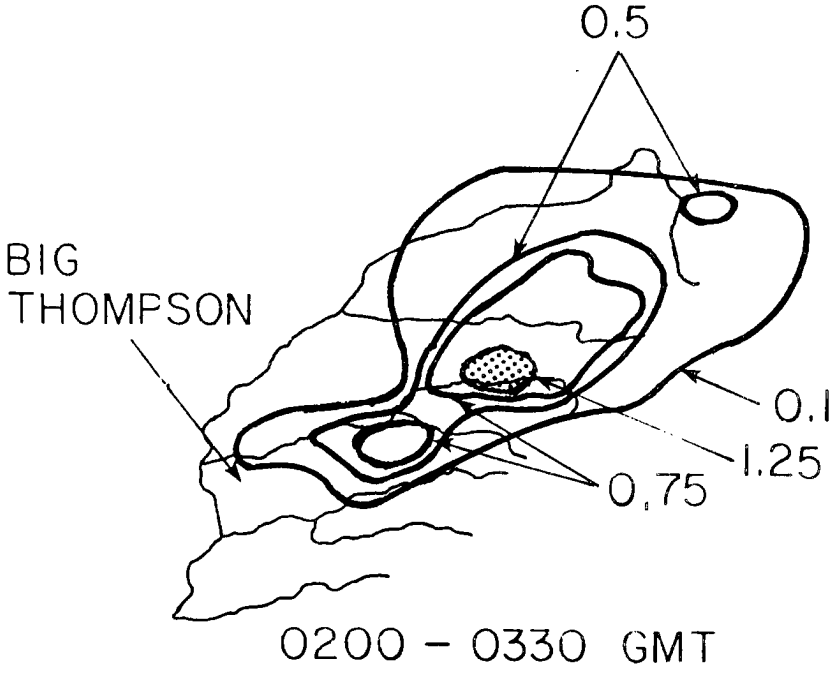

Figure 4-17 Satellite-derived half-hourly isohyet analysis (in), 0200-0330 GMT, 1 August 1976.

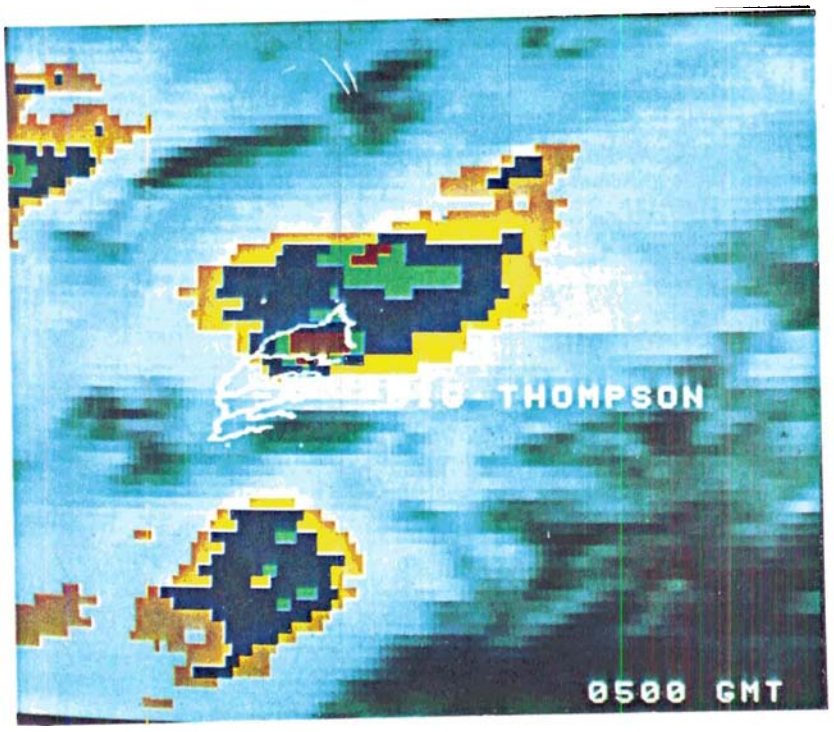

Figure 4-18 Infrared image 1 August 1976 0500 GMT with drainage area overlay.

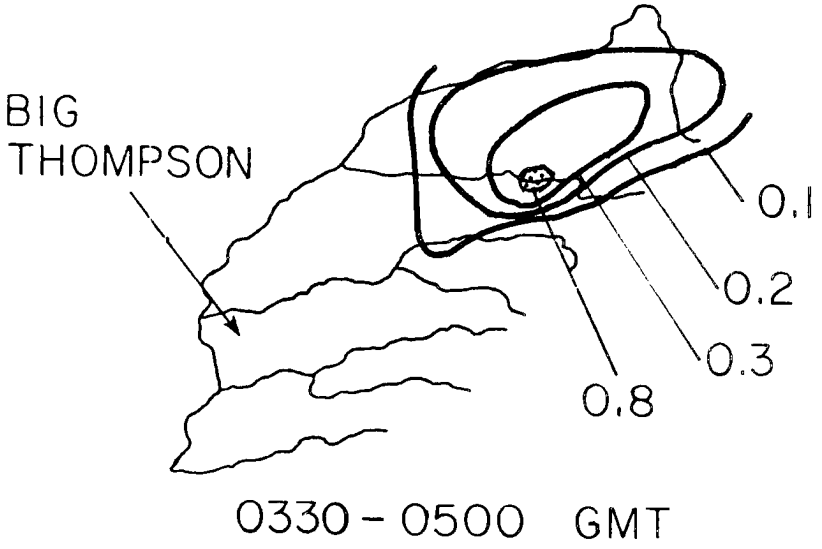

Figure 4-19 Satellite-derived half-hourly isohyet analysis (in), 0330-0500 GMT, 1 August 1976.

the heaviest precipitation areas displayed in the radar echo figures.

Figures 4-11, 4-13, 4-15, 4-17 and 4-19 show the half-hourly isohyets derived from the modified Scofield-Oliver technique. The shaded areas include precipitation enhancement of 12.7 mm (0.5 in) due to the presence of overshooting domes or higher cirrostratus. Figure 4-17 is the half-hourly rainfall rate obtained from the 0200 and 0330 GMT satellite images. Since no images were available for 0230 and 0300 GMT and the radar showed heavy precipitation over the Big Thompson Basin through 0300 GMT, the 19 mm (0.75 in) isohyet over the Big Thompson was enhanced by 12.7 mm (0.5 in) through 0300 GMT. Physically, it was reasoned that the intensive updrafts causing the overshooting dome continued through 0300 GMT but were slackening by the 0330 GMT image. Again, the heaviest precipitation areas correlated well with the radar display.

The isohyetal analyses were averaged to allow for changes in precipitation intensity and cell movement. The resulting hourly and cumulative area-averaged rainfall rates were compared to the results obtained by Woodley, et al. (1978) and ground truth calculated from gage-adjusted radar provided by Caracena, et al. (1978). Figures 4-20 and 4-21 show hourly and cumulative area-averaged rainfall for the Big Thompson drainage area. The modified Scofield-Oliver technique estimations computed in this study compare quite favorably with the ground truth on an hourly basis. Also, the total of 61.94 mm (2.44 in) compared to the ground truth 68.5 mm (2.70 in) represents an error of only 9.6 percent. Figures 4-22 and 4-23 show the hourly and cumulative area-averaged rainfall for the Big Thompson, Little Thompson, and St. Vrain drainage areas. The latter two are located below the Big Thompson

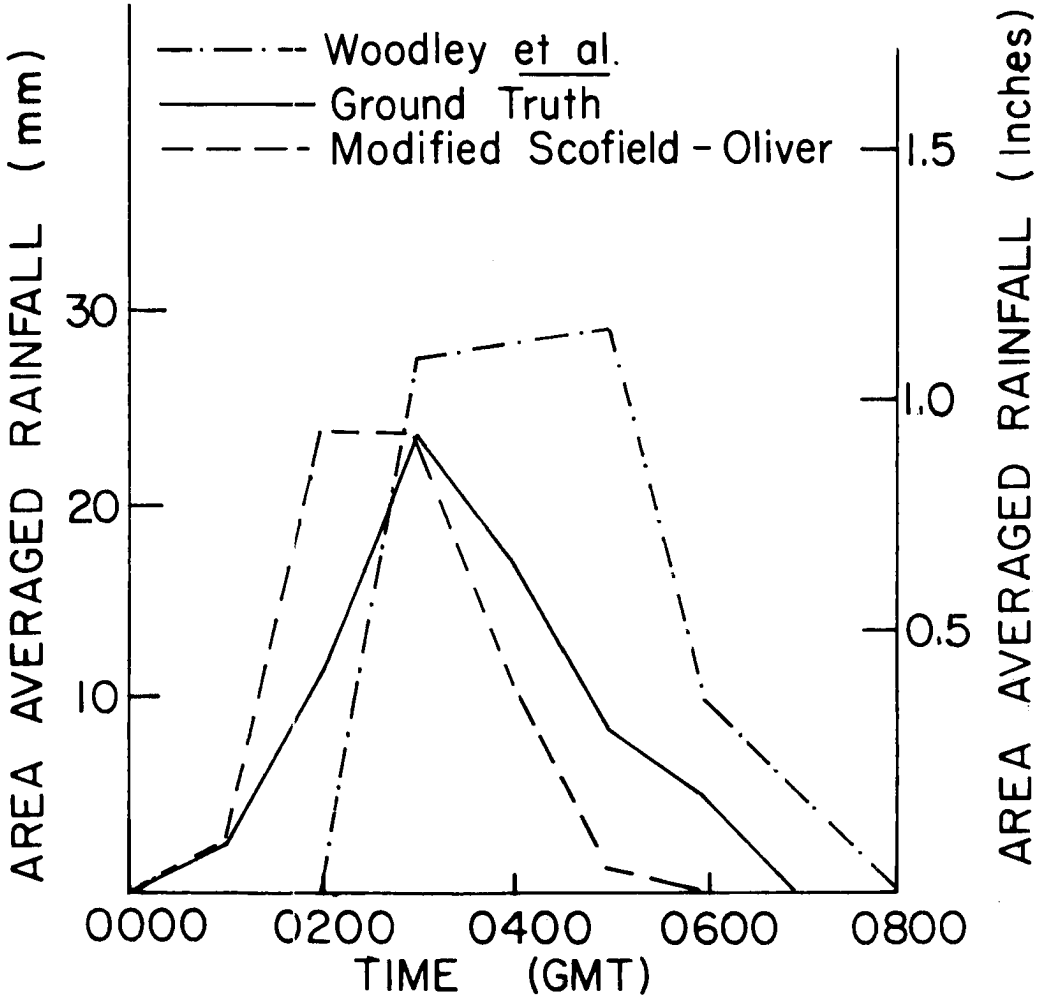

Figure 4-20 Hourly area-averaged rainfall for the Big Thompson Basin on 1 August 1976.

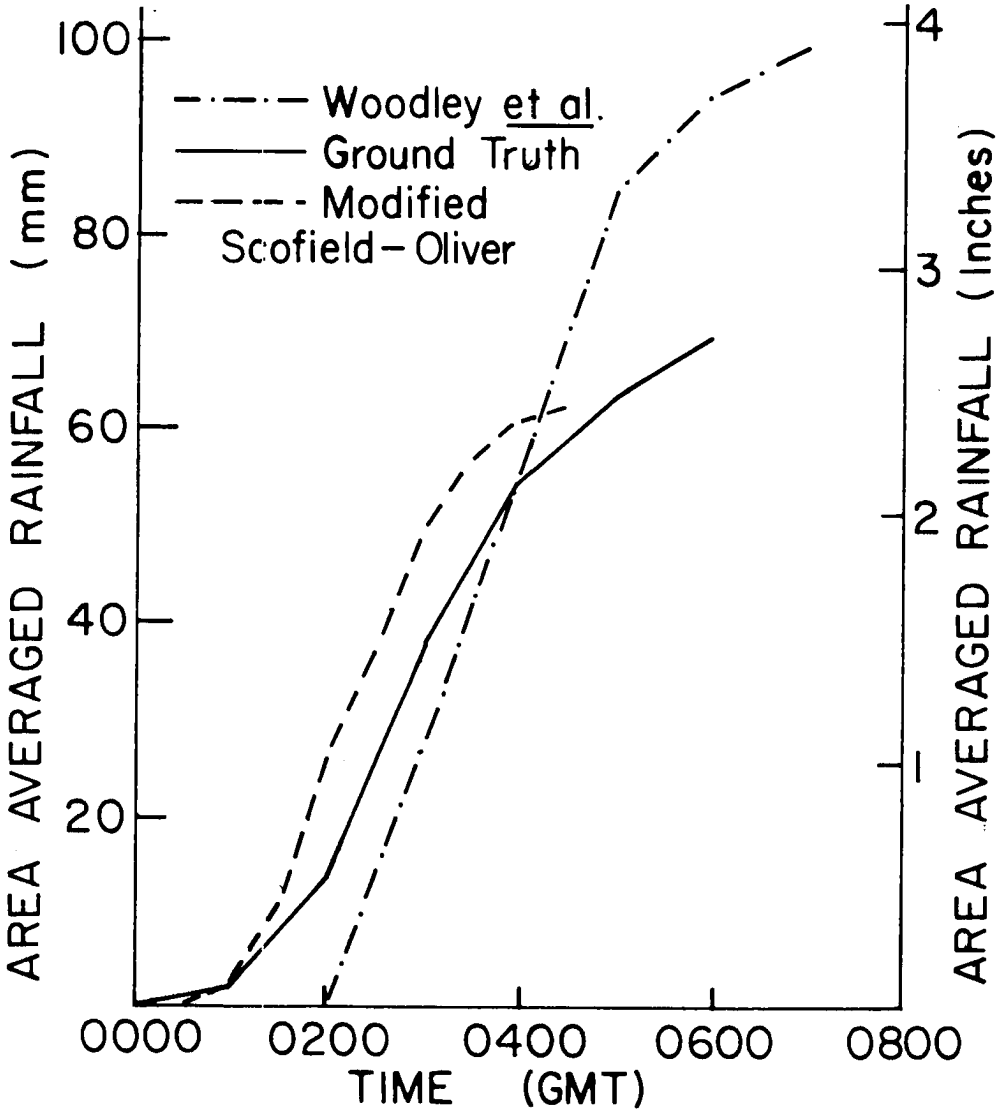

Figure 4-21 Cumulative area-averaged rainfall for the Big Thompson Basin on 1 August 1976.

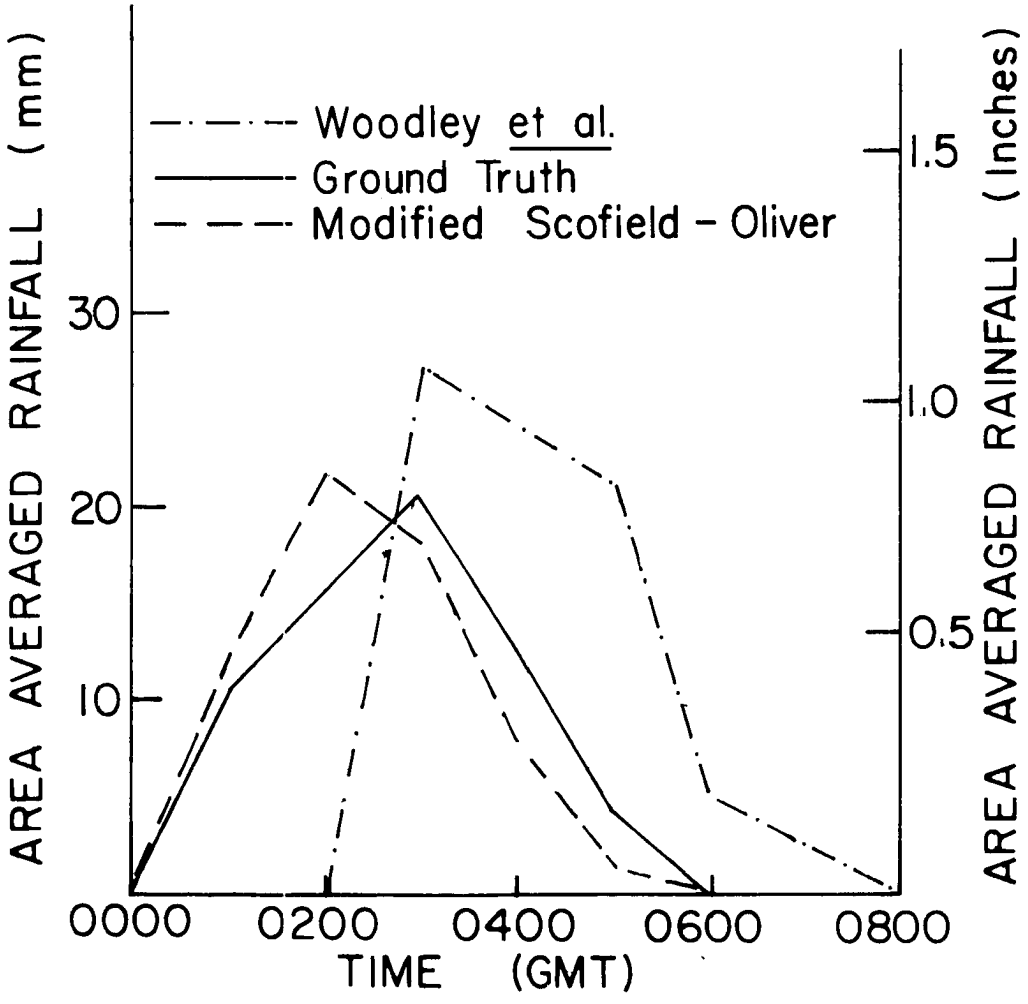

Figure 4-22 Hourly area-averaged rainfall for the Big Thompson, Little Thompson and St. Vrain Drainage Basins on 1 August 1976.

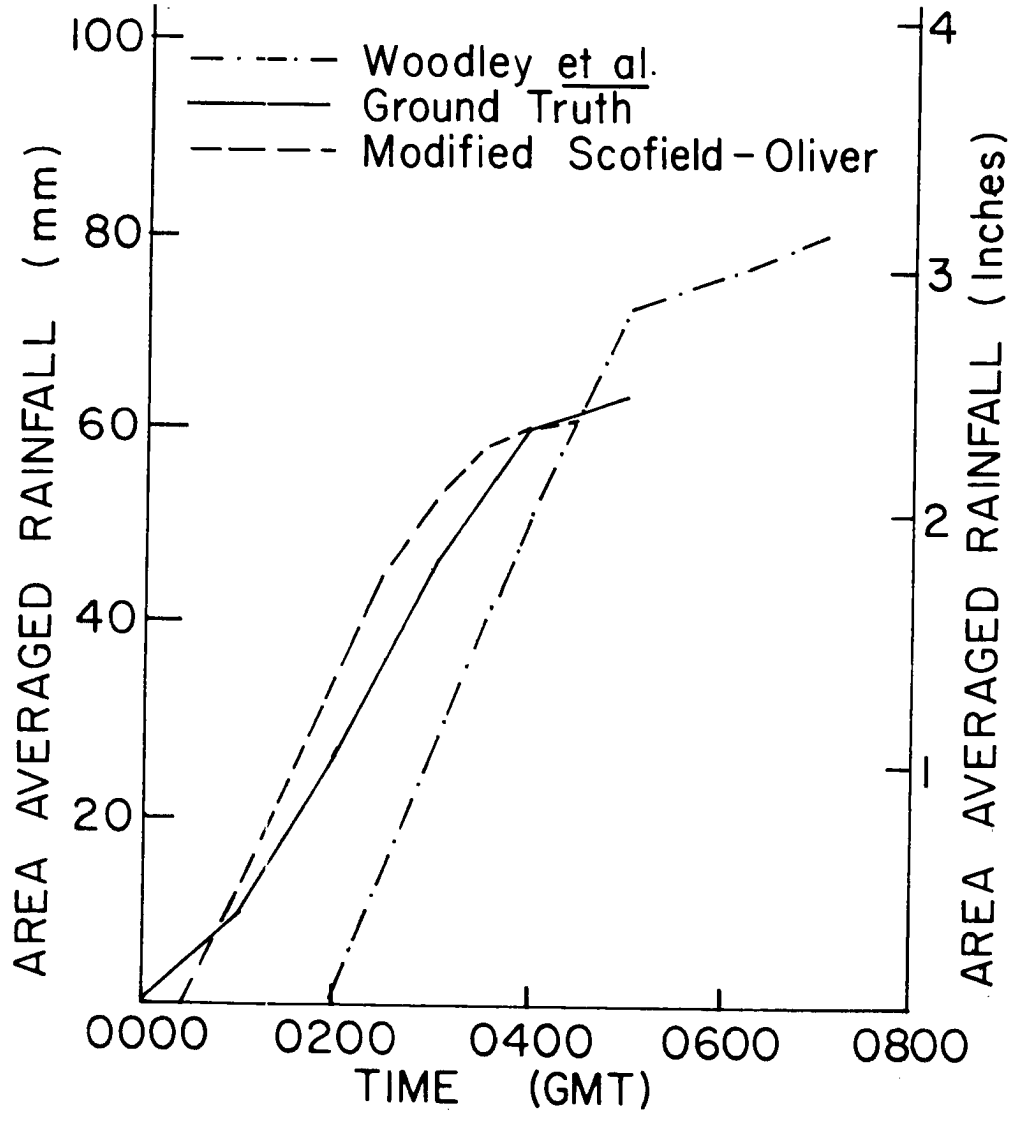

Figure 4-23 Cumulative area-averaged rainfall for the Big Thompson, Little Thompson, and St. Vrain Drainage Basins on 1 August 1976.

Basin on the grid. Again, the correlation is quite good and the total accumulation of 61.4 mm (2.42 in) is only in error by 3.6 percent when compared to the ground truth of 63.7 mm (2.51 in).

5.0 SUMMARY AND CONCLUSIONS

The most important aspect in the prediction of flash flooding is the determination and prediction of rainfall amounts over the area concerned. Identification of meteorological conditions favorable for heavy rainfall can indicate regions where the potential for flash flooding exists. Favorable meteorological conditions for the Big Thompson flood as outlined by Maddox, et al. (1977) were:

1. Moist conditionally unstable air advected into the region.
2. Orographic lifting triggered the thunderstorm activity.
3. Weak south-southwesterly winds aloft allowed the thunderstorm complex to remain nearly stationary.

Satellite images can further pinpoint locations for heavy rainfall. Purdom (1976), using high resolution visible data, showed that intense convective activity develops at the intersection of convective lines or at a merger of a convective line and thunderstorm produced "arc" cloud. In this study, lower resolution IR images were used to predict the location of the Big Thompson thunderstorm complex at the intersection of the frontal and orographic convective lines.

An important aspect in the determination of rainfall over a specific area is the absolute navigation of the precipitating clouds. A computer program by Smith and Phillips (1972) can satisfactorily navigate satellite images to specific landmarks. The navigation program coupled with the All Digital Video Imagery System for Atmospheric Research (ADVISAR) were used to superimpose a grid of the drainage areas studied over the satellite images. The overlay capability could be used to superimpose radar echoes, gage reports, etc., that would aid in the interpretation of the satellite image. The navigation of overlay was

corrected for the error caused by the satellite sensing cloud tops. Over the Big Thompson Basin, this error would displace 20 km (65,500 ft) MSL cloud tops by almost 30 km (18.6 mi) away from the satellite sub-point.

The Scofield-Oliver rainfall estimation technique used on the Big Thompson proved to be quite accurate after modification. The assumption that only the coldest 15 percent of the cloud as defined by the 242^{o}K isotherm was precipitating proved quite viable when compared to the Limon radar presentations. Additionally, rainfall amplification of 12.7 mm (0.5 in) was added to the initial estimate for areas under over-shooting domes. The overshooting domes are composed of smaller over-shooting turrets and are indicative of strong vertical motion as shown by Fujita (1972, 1974) and Shenk (1974). The persistent overshooting domes correlated well with the areas of heaviest rainfall as determined by the Limon radar. The ADVISAR proved invaluable in this scheme as the color enhanced 1^{o}K resolution allowed for a more accurate determination of cloud top isotherms which led to more precise rainfall isohyets.

Hourly and cumulative area-averaged precipitation amounts obtained by the modified Scofield-Oliver technique were in good agreement with ground truth in the Big Thompson drainage Basin. The total of 61.94 mm (2.44 in) was only in error by 9.6 percent when compared to the ground truth as determined by gage-adjusted radar of 68.5 mm (2.70 in).

Use of the modified Scofield-Oliver precipitation technique on the ADVISAR can indicate areas of heavy rainfall on a real-time basis. However, this technique should be used on additional studies to further prove its reliability.

REFERENCES

Brown, M. L., 1978: Digital video manipulation of satellite data. Preprint of Fourth Symposium on Meteorological Observations and Instrumentation, AMS, Denver, Colorado, 207-211.

Caracena, F., R. A. Maddox, L. R. Hoxit, and D. F. Chappell, 1978: Mesoanalysis of the Big Thompson storm. Submitted to Mon. Wea. Rev.

Fujita, T. T., 1972: Tornado occurences related to overshooting cloud-top heights as determined from ATS pictures. SMRP Research Paper 97, University of Chicago, 32p.

Fujita, T. T., 1974: Overshooting thunderheads observed from ATS and learjet. SMRP Research Paper 117, University of Chicago, 29p.

Griffith, C. G. and W. L. Woodley, 1973: On the variation with height of the top brightness of precipitating convective clouds. J. Appl. Meteor., 12, 1986-1989.

Griffith, C. G., W. L. Woodley, S. Browner, J. Teijerio, M. Maier, D. W. Martin, J. Stout, and D. N. Sikdar, 1976: Rainfall estimation from geosynchronous satellite imagery during daylight hours. NOAA Technical Report ERL356-WMPO 7, 106p.

Grozier, R. U., J. F. McCain, L. F. Lang, and D. C. Merriman, 1976: The Big Thompson river flood of July 31 - 1 August, 1976. Larimer County, Colorado, U.S.G.S. and Colorado Water Conservation Board Flood Information Report, Denver, 78p.

Hughes, L. A. and L. L. Longsdorf, 1978: Guidelines for flash flood and small tributary flood prediction. NOAA Technical Memorandum NWS CR-58, 7p.

Maddox, R. A., F. Caracena, L. R. Hoxit and C. F. Chappell, 1977: Meteorological aspects of the Big Thompson flash flood of 31 Jul 1976. NOAA Technical Report ERL 388-APCL 41, 83p.

Martin, D. W. and W. D. Scherer, 1973: Review of satellite rainfall estimation methods. Bull. Amer. Meteor. Soc., 54, 661-674.

Martin, D. W. and D. N. Sikdar, 1973: Calibration of ATS-3 images for quantitative precipitation estimation. Report to NOAA, Contract 03-3-022-18, Space Science and Engineering Center, Madison, Wisconsin, 12p.

Martin, D. W. and D. N. Sikdar, 1974: Rainfall estimation from satellite images. Report to NOAA, Contract 03-4-022-22, Space Science and Engineering Center, Madison, Wisconsin, 8p.

McKowan, P. O., 1975: Data processing plan for Synchronous Meteorological and Geostationary Operational Environmental Satellites (SMS/GOES). Goddard Space Flight Center X-565-75-275, Greenbelt, Maryland, 276p.

Miller, R. C., 1972: Notes on analysis and severe-storm forecasting procedures of the Air Force Global Weather Central. Air Weather Service Technical Report 200, 190p.

Pryor, 1978: Measurement of thunderstorm cloud-top parameters using high-frequency satellite imagery. Master's Thesis, Colorado State University, Fort Collins, Colorado, 101p.

Purdom, J. F. W., 1973: Satellite imagery and the mesoscale convective forecast problem. Preprint of Eighth Conf. Severe Local Storms, AMS, Denver, Colorado, 244-251.

Purdom, J. F. W., 1974: Satellite imagery applied to the mesoscale surface analysis and forecast. Preprint of Fifth Conf. Weather Forecasting and Analysis, AMS, St. Louis, Missouri, 63-68.

Purdom, J. F. W., 1976: Some uses of high-resolution GOES imagery in the mesoscale forecasting of convective and its behavior. Mon. Wea. Rev., 104, 1474-1483

Reynolds, D. and T. H. Vonder Haar, 1973: A comparison of radar-determined cloud height and reflected solar radiance measured from the geosynchronous satellite ATS-3. J. Appl. Meteor., 12, 1082-1085.

Scofield, R. A., 1978: Using satellite imagery to estimate rainfall during the Johnstown rainstorm. Preprint of Conf. on Flash Floods: Hydrometeorolcgical Aspects, AMS, Los Angeles, California, 181-189.

Scofield, R. A. and V. J. Oliver, 1977a: A scheme for estimating convective rainfall from satellite imagery. NOAA/NESS Technical Memorandum 86, 47p.

Scofield, R. A. and V. J. Oliver, 1977b: Using satellite imagery to estimate rainfall from two types of convective systems. Preprint of Tenth Technical Conf. on Hurricanes and Tropical Meteorology, Boston, Massachusetts, 204-211.

Shenk, W. E., 1974: Cloud top height variability of strong convective cells. J. Appl. Meteor., 13, 917-922.

Simons, D. B., J. D. Nelson, E. R. Reiter, and R. L. Barkau, 1977: Report on Big Thompson flood. Prepared for Committee on Natural Disasters, Commission on Sociotechnical Systems, National Research Council, Washington, District of Columbia, 129p.

Simpson, J. and W. L. Woodley, 1971; Seeding cumulus in Florida: new 1970 results. Science, 172, 117-126.

Smith, E. A. and D. R. Phillips, 1972: Automated cloud tracking using precisely aligned digital ATS pictures. IEEE Transactions on Computers, C-21, 517-519.

Woodley, W. L., C. G. Griffith, J. Griffin, and J. Augustine, 1978: Satellite rain estimation in the Big Thompson and Johnstown flash floods. Preprint of Conf. on Flash Floods: Hydro-meteorological Aspects, AMS, Los Angeles, California, 44-51.

Woodley, W. L. and R. I. Sax, 1976: The Florida area cumulus experiment: rationale, design, procedures, results and future course, NOAA Technical Report ERL 354-WMP06, 204p.

ACKNOWLEDGEMENTS

For their assistance in the preparation and review of this paper, I wish to thank my committee members, Dr. Thomas H. Vonder Haar, Dr. Elmar R. Reiter, and Dr. Everett V. Richardson. Special thanks to the National Space Science Data Center and the National Oceanic and Atmospheric Administration Environmental Research Laboratory for the digitized satellite data used in this study. This research was supported by the Air Force Institute of Technology.

My appreciation to Pauline J. Martin for drafting of figures, Janice P. Root for typing this manuscript and to Mark J. Whitcomb for computer programming assistance.

APPENDIX A

SATELLITE IMAGE REGISTRATION

Infrared satellite data for 31 July - 1 August 1976 was registered by landmark matching. The image registration is presented in Table A-1. The relative line and element shifts are those necessary to collocate any two images.

TABLE A-1

Satellite Image Registration

Date	Time (GMT)	Shift Lines	Shift Elements
31 July 1976	2000	-3	-1
	2030	-3	-1
	2045	-3	-1
	2100	-59	0
	2130	-5	+2
	2200	-70	+2
	2230	-27	+2
	2300	-4	+7
	2330	-4	+3
1 Aug 1976	0000	-1	-1
	0100	-2	0
	0130	0	0
	0200	0	-6
	0330	0	-4
	0500	+1	-4
	0630	+1	-6
	0800	+2	-9
	0830	+1	-10

BIBLIOGRAPHIC DATA SHEET	1. Report No. CSU-ATSP-300	2.	3. Recipient's Accession No.
4. Title and Subtitle Estimation of Big Thompson Flood Rainfall Using Infrared Satellite Imagery			5. Report Date December 1978 6.
7. Author(s) Dennis E. Bielicki and Thomas H. Vonder Haar			8. Performing Organization Rept. No. 300
9. Performing Organization Name and Address Atmospheric Science Department Colorado State University Fort Collins, Colorado 80523			10. Project/Task/Work Unit No. 11. Contract/Grant No.
12. Sponsoring Organization Name and Address Air Force Institute of Technology Wright Patterson Air Force Base Ohio 45433			13. Type of Report & Period Covered 14.

15. Supplementary Notes

16. Abstracts

During the evening hours of 31 July 1976 heavy precipitation fell along the Colorado Front Range resulting in flash flooding in the Big Thompson Canyon causing the death of 139 people with 35.5 million dollar damage. This report utilizes GOES-1 infrared (IR) imagery to estimate the heavy convective precipitation during the Big Thompson Flood.

Analysis of the IR imagery prior to the Big Thompson storm showed that the thunderstorm complex formed at the intersection of frontal and orographic convective lines. A technique is developed to overlay the drainage basins onto the satellite imagery using the All Digital Video Imaging System for Atmospheric Research (ADVISAR) which included corrections due to the satellite sensing cloud tops.

The Scofield-Oliver satellite-derived precipitation estimation scheme was modified to reduce the precipitating portion of the cloud to 15 percent of the cloud defined by the 242° K isotherm. IR imagery along was used to identify overshooting domes which correlated well with areas of heavy precipitation. The computed area averaged precipitation for the Big Thompson Basin was 9.6 percent less than ground truth. Digital-video manipulation on the ADVISAR can indicate areas of heavy precipitation for IR satellite data on a real time basis.

17. Key Words and Document Analysis. 17a. Descriptors

Flash flooding
Big Thompson Canyon
Infrared satellite imagery
Satellite precipitation estimation

17b. Identifiers/Open-Ended Terms

17c. COSATI Field/Group

18. Availability Statement	19. Security Class (This Report) UNCLASSIFIED	21. No. of Pages 62
	20. Security Class (This Page) UNCLASSIFIED	22. Price